

000 DocPruner: A STORAGE-EFFICIENT FRAMEWORK 001 FOR MULTI-VECTOR VISUAL DOCUMENT RETRIEVAL 002 VIA ADAPTIVE PATCH-LEVEL EMBEDDING PRUNING 003 004

006 **Anonymous authors**

007 Paper under double-blind review

011 ABSTRACT

013 Visual Document Retrieval (VDR), the task of retrieving visually-rich document
014 pages using queries that combine visual and textual cues, is crucial for numerous
015 real-world applications. Recent state-of-the-art methods leverage Large Vision-
016 Language Models (LVLMs) in a multi-vector paradigm, representing each doc-
017 ument as patch-level embeddings to capture fine-grained details. While highly
018 effective, this approach introduces a critical challenge: *prohibitive storage over-*
019 *head*, as storing hundreds of vectors per page makes large-scale deployment costly
020 and impractical. To address this, we introduce DocPruner, **the first framework**
021 **to employ adaptive patch-level embedding pruning for VDR** to effectively re-
022 duce the storage overhead. DocPruner leverages the intra-document patch atten-
023 tion distribution to dynamically identify and discard redundant embeddings for
024 each document. This adaptive mechanism enables a significant 50-60% reduction
025 in storage for leading multi-vector VDR models with negligible degradation in
026 document retrieval performance. Extensive experiments across more than ten rep-
027 resentative datasets validate that DocPruner offers a robust, flexible, and effective
028 solution for building storage-efficient, large-scale VDR systems.

030 1 INTRODUCTION

032 Visual Document Retrieval (VDR), the task of retrieving relevant document pages based on a query
033 that leverages both visual and textual cues, is of paramount importance in numerous real-world
034 applications, from e-commerce product searches to educational resource discovery (Ding et al.,
035 2024; Zheng et al., 2025; Wang et al., 2025b). In contrast to traditional text retrieval, VDR presents
036 a greater challenge as it must interpret not only the textual content but also the complex layouts,
037 tables, figures, and other visual elements that convey critical information (Abootorabi et al., 2025;
038 Mei et al., 2025). Consequently, this intricate task has garnered increasing attention within the
039 information retrieval community in recent years, driving innovation beyond text-centric paradigms.

040 The methodology for VDR has undergone a significant paradigm shift. Early approaches were
041 predominantly **OCR-based**, involving the extraction of text from document images, which was
042 then indexed by conventional text retrievers (Zhang et al., 2024a; Hegghammer, 2022), as shown
043 in Figure 1 (a). However, these methods are often brittle and error-prone, frequently *fails to*
044 *preserve the vital layout and structural relationship inherent in the visual representation* (Most et al.,
045 2025; Guo et al., 2025). With the recent advent of Large Vision-Language Models (LVLMs) and
046 their dramatically enhanced visual understanding capabilities (Caffagni et al., 2024), the research
047 community has begun to explore **LVLM-based** methods, which have demonstrated state-of-the-art
048 retrieval performance (Macé et al., 2025; Günther et al., 2025; Dong et al., 2025; Tanaka et al.,
049 2025). These methods generally fall into two categories: one that encodes an entire document page
050 and the query into single, holistic embeddings (*i.e.*, page-level retrieval) (Zhang et al., 2024c; Liu
051 et al., 2025b; Jiang et al., 2024b; Meng et al., 2025), and another that represents a document as
052 multiple patch-level embeddings and the query as multiple token-level embeddings, as illustrated
053 in Figure 1 (b). The former approach, while simple, often *fails to capture the fine-grained details*
necessary for understanding complex documents, leading to suboptimal performance. As a result,
the latter patch-level retrieval has emerged as the preferred paradigm for leading models.

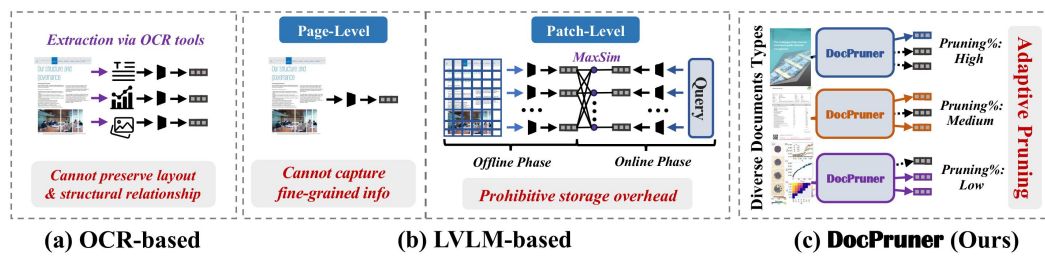


Figure 1: The illustration of comparison between OCR-based (a) & LVLM-based (b) paradigms for VDR, and DocPruner (c), a novel framework to adaptively prune the patch-level embeddings for diverse document types.

The ascent of the patch-level retrieval paradigm is primarily attributed to the advantages of multi-vector retrieval, a technique pioneered by ColBERT-style late interaction (Khattab & Zaharia, 2020). The core mechanism of this approach involves a MaxSim operation, where for each query token embedding, the maximum similarity score against all patch embeddings of a document is computed, and these scores are then aggregated to determine relevance. The VDR field first witnessed the successful application of this paradigm with ColPali (Faysse et al., 2024), which spurred a wave of subsequent works that further refined and enhanced the performance of multi-vector VDR (NomadicAI, 2025; Günther et al., 2025; Xu et al., 2025a; Karlinsky et al., 2025). However, despite its effectiveness, *the multi-vector approach suffers from a critical efficiency bottleneck: prohibitive storage overhead*. Storing hundreds or even thousands of embedding vectors for every single document makes large-scale deployment costly and challenging (Ma et al., 2025).

To address this critical challenge, we introduce **DocPruner**, the **first framework to successfully employ adaptive pruning in the context of VDR** to significantly alleviate storage overhead, as shown in Figure 1 (c). The core of DocPruner is an elegant yet powerful mechanism that leverages the patch-level attention score distribution within a single document to perform adaptive pruning of its patch embeddings. This allows the framework to dynamically adjust the pruning ratio for different documents, achieving a 50-60% reduction in patch embeddings for several state-of-the-art multi-vector models with negligible performance degradation. While some prior works have explored efficiency optimizations for multi-vector VDR, they are often constrained by pre-defined pruning rates or fixed thresholds (Cheng et al., 2024a; Ma et al., 2025; Tmamna et al., 2024), which lack the adaptability required for diverse, real-world visual documents. We believe that the design philosophy of DocPruner, which enables robust performance even for diverse models and datasets, ensures its flexibility and extensibility for practical, large-scale multimodal retrieval applications.

Our contributions can be summarized as follows:

- ① Pioneering Pruning for VDR.** We propose DocPruner, the first framework to introduce an adaptive pruning mechanism to the VDR domain. It achieves a substantial 50-60% average patch pruning rate with near-lossless performance, effectively mitigating the storage overhead of top-performing multi-vector VDR models.
- ② Adaptive Property for Diverse Documents.** The adaptive nature of DocPruner allows it to dynamically tailor the pruning ratio for different types of visual documents, a feature that is particularly crucial in real-world scenarios where document formats and information densities vary widely.
- ③ Extensive Experimental Validation.** We conduct comprehensive experiments on diverse and even multilingual VDR benchmarks, demonstrating the effectiveness and robustness of DocPruner when integrated with multiple leading multi-vector retrieval models in the community.

2 RELATED WORK

2.1 VISUAL DOCUMENT RETRIEVAL

Visual Document Retrieval (VDR) aims to retrieve relevant visually-rich documents based on visual representations, a paradigm that has garnered significant attention from the research community (Zheng et al., 2025; Mei et al., 2025; Zhang et al., 2025b). Previous **OCR-based methods** rely on document parsing to extract textual content (Xiao et al., 2024; Wang et al., 2023; Karpukhin et al., 2020), a process that can *lose critical layout information and fail to interpret non-textual components*. Consequently, the field has rapidly evolved from early OCR-plus-retriever pipelines to

108 a paradigm leveraging powerful VLMs as OCR-free retriever backbones. By treating documents as
 109 images, VDR systems can preserve this vital structural and visual integrity, enabling a “what-you-
 110 see-is-what-you-get” retrieval mechanism that aligns with human perception (Ma et al., 2024).

111 These **VLM-based methods** primarily fall into two categories: efficient but less detailed page-level
 112 retrieval, and the more powerful patch-level retrieval. **Page-level retrievers**, such as DSE (Ma et al.,
 113 2024), GME (Zhang et al., 2024c) and UniSE (Liu et al., 2025b), encode an entire document page
 114 into a single, compact embedding. While efficient, this approach may *lose fine-grained details crucial*
 115 *for specific queries*. State-of-the-art **patch-level retrievers** (e.g., ColPali (Faysse et al., 2024),
 116 ColQwen (Faysse et al., 2024), ColNomic (NomicAI, 2025), Jina Embeddings v4 (Günther et al.,
 117 2025), and Llama Nemoretriever Colembed (Xu et al., 2025a)) achieve superior performance by
 118 generating fine-grained, multi-vector representations per page, yet this introduces a critical bottle-
 119 neck due to *prohibitive storage and computational overhead*. Our proposed **DocPruner** directly
 120 addresses this pain point by proposing a solution to adaptively reduce the storage footprint of patch-
 121 level embeddings, thereby making high-performance VDR more practical and scalable.

122 2.2 MULTI-VECTOR RETRIEVAL

124 Multi-vector retrievers, also known as late-interaction models (Khattab & Zaharia, 2020; Ji et al.,
 125 2024), computes relevance by first independently encoding queries and documents into sets of token-
 126 level embeddings and then performing fine-grained similarity calculations. Formally, given a query
 127 q and a document d with L_1 and L_2 tokens respectively, they are encoded into embedding matrices
 128 $\mathbf{Q} = (\mathbf{q}_1, \dots, \mathbf{q}_{L_1}) \in \mathbb{R}^{P \times L_1}$ and $\mathbf{D} = (\mathbf{d}_1, \dots, \mathbf{d}_{L_2}) \in \mathbb{R}^{P \times L_2}$, where P is the embedding
 129 dimension. The final score is derived from their token-wise similarity matrix $\mathbf{S} = \mathbf{Q}^\top \mathbf{D}$. For
 130 instance, ColBERT model (Khattab & Zaharia, 2020) computes the score via a MaxSim operation:

$$131 \quad s(q, d) = \sum_{i=1}^{L_1} \max_{j=1}^{L_2} \mathbf{q}_i^\top \mathbf{d}_j. \quad (1)$$

134 Building on this foundation, ColBERTv2 (Santhanam et al., 2021) introduced a centroid-based
 135 method to compress token embeddings for greater storage efficiency. PLAID (Santhanam et al.,
 136 2022) further optimized this by using centroid interactions for efficient pruning of low-scoring
 137 documents. Other approaches have focused on reducing the number of stored vectors: XTR (Lee et al.,
 138 2023) trains the model to prioritize and retrieve only key document tokens, Acquavia et al. (2023)
 139 remove embeddings of less impactful tokens, and Clavié et al. (2024) cluster similar token embed-
 140 dings at indexing time to reduce the total vector count. Recently, MUVERA (Jayaram et al., 2024)
 141 proposed using Fixed Dimensional Encodings (FDEs) to approximate the multi-vector similarities,
 142 enabling efficient retrieval. Despite their effectiveness, a primary limitation of these text-based
 143 multi-vector models is their *significant storage overhead*, which scales linearly with the number of
 144 document tokens (L_2), resulting in a storage cost of $O(P \times L_2)$ per document, a substantial increase
 145 compared to $O(P)$ cost of single-vector models (MacAvaney et al., 2025; Ji et al., 2024).

146 The concept of multi-vector retrieval has been extended to VDR, leveraging the fine-grained inter-
 147 action capabilities to better align textual queries with visual content (Plale et al., 2025; Xu et al.,
 148 2025b). Pioneering this direction, ColPali (Faysse et al., 2024) adapted the ColBERT framework
 149 by using PaliGemma-3B model (Beyer et al., 2024) to generate multi-vector embeddings directly
 150 from document images. Subsequently, Llama Nemoretriever Colembed (Xu et al., 2025a) further
 151 advanced this paradigm by modifying Llama-3.2-3B (Grattafiori et al., 2024) with bidirectional atten-
 152 tion and employing a two-stage training strategy to achieve state-of-the-art performance on the
 153 ViDoRe benchmark. More recently, Jina Embeddings v4 (Günther et al., 2025) proposed a unified
 154 Qwen2.5-VL (Bai et al., 2025) architecture that supports both single-vector and multi-vector out-
 155 puts, utilizing LoRA adapters for task-specific optimization. However, the storage overhead problem
 156 persists in these visual models, which remains a critical challenge that **DocPruner** aims to address.

157 More related work can be seen in Appendix A.

158 3 METHODOLOGY

160 In this section, we first formalize the setting of multi-vector VDR in (▷ Section 3.1). We then
 161 introduce our proposed framework, **DocPruner**, detailing its mechanism for adaptive patch-level

embedding pruning in (▷ Section 3.2). Finally, we establish a theoretical foundation rooted in information theory to justify its efficacy in (▷ Section 3.3).

3.1 TASK FORMULATION

The task of VDR is to retrieve a ranked list of relevant document pages from a large corpus $\mathcal{C} = \{d_1, d_2, \dots, d_{|\mathcal{C}|}\}$ for a given textual query q . In the context of multi-vector VDR (Fayse et al., 2024), both queries and documents are represented by sets of embedding vectors.

Let a query q be a sequence of L_q textual tokens. A VLM-based encoder, denoted as $\Phi(\cdot)$, maps this query into a set of token-level embeddings $\mathbf{Q} = \{\mathbf{q}_i\}_{i=1}^{L_q}$, where each $\mathbf{q}_i \in \mathbb{R}^P$ and P is the embedding dimension. Similarly, a document page d is first rendered as an image and then processed by the VLM encoder $\Phi(\cdot)$, which divides the image into a grid of patches. This process yields a set of L_d patch-level embeddings $\mathbf{D} = \{\mathbf{d}_j\}_{j=1}^{L_d}$, where each $\mathbf{d}_j \in \mathbb{R}^P$.

Following the late-interaction paradigm (Khattab & Zaharia, 2020; Santhanam et al., 2021), the relevance score $s(q, d)$ is computed via a MaxSim operation as defined in Equation 1. The primary challenge is the storage overhead associated with this representation. Storing the full set of embeddings \mathbf{D} for every document results in a cost of $O(L_d \times P)$ per page, which is prohibitive for large-scale corpora. Our objective is to generate a pruned set of document embeddings $\mathbf{D}' \subset \mathbf{D}$ such that its size, $L'_d = |\mathbf{D}'|$, is significantly smaller than L_d ($L'_d \ll L_d$), thereby substantially reducing the storage cost to $O(L'_d \times P)$ while preserving retrieval performance.

3.2 THE DocPruner FRAMEWORK

DocPruner is a lightweight, plug-and-play framework applied during the offline indexing phase. It is designed around two core principles: being **query-agnostic** to enable offline processing and **document-adaptive** to handle the diverse nature of visual documents. The framework systematically identifies and discards redundant or less informative patch embeddings without requiring any model retraining. The process involves three main steps: quantifying patch importance, applying an adaptive threshold, and scoring with the pruned embeddings. See pseudocode in Section B.

3.2.1 QUANTIFYING PATCH IMPORTANCE VIA GLOBAL TOKEN ATTENTION

The central challenge of offline pruning is to *estimate the importance of each patch without access to a query*. We need a reliable, intrinsic signal of salience. Our key insight is that a VLM, in the process of understanding a document image, already computes such a signal. Specifically, we leverage the attention mechanism directed towards a **global token**. A global token is a special token whose final hidden state is trained to aggregate and summarize information from the entire input sequence. Its representation must encapsulate the document’s overall semantics.

In our framework, we use the end-of-sequence [EOS] token as the default global token, a common and effective choice in many VLM architectures. We extract the attention weights from the final Transformer layer, as this layer captures the most abstract and semantically rich relationships.

Formally, let $\mathbf{A}^{(L)}$ be the attention weights from the final layer L . After averaging across all H attention heads to create a smooth, robust attention map ($\bar{\mathbf{A}}_{i,j}^{(L)} = \frac{1}{H} \sum_{h=1}^H \mathbf{A}_{h,i,j}^{(L)}$), we define the importance score $I(\mathbf{d}_j)$ for the j -th patch as the attention it receives from the global token:

$$I(\mathbf{d}_j) = \bar{\mathbf{A}}_{\text{global},j}^{(L)}. \quad (2)$$

This process yields a vector of importance scores $\mathcal{I}_d = \{I(\mathbf{d}_j)\}_{j=1}^{L_d}$ for each document, which serves as the foundation for our adaptive pruning.

3.2.2 ADAPTIVE THRESHOLDING FOR PRUNING

Naive pruning strategies, such as using a fixed pruning ratio or a global threshold, are ill-suited for VDR. Visual documents exhibit vast heterogeneity in information density—a sparse title page has very different characteristics from a dense, text-filled page. A fixed strategy would either over-prune the dense page, losing critical information, or under-prune the sparse page, retaining useless

background patches. **DocPruner**'s adaptive thresholding directly addresses this by tailoring the pruning decision to the statistical properties of each individual document.

For a given document d with L_d patch embeddings, we have a corresponding vector of importance scores $\mathcal{I}_d = \{I(\mathbf{d}_j)\}_{j=1}^{L_d}$. Our method computes a document-specific threshold by leveraging the first two statistical moments of these scores. First, we define the **mean importance** μ_d , which establishes a baseline salience level for the document's patches. A high mean suggests the document is generally information-rich. It is formally calculated as:

$$\mu_d = \frac{1}{L_d} \sum_{j=1}^{L_d} I(\mathbf{d}_j). \quad (3)$$

Second, we compute the **standard deviation** σ_d , which measures the dispersion of importance scores. A high standard deviation indicates that a few patches are exceptionally important compared to the rest, a hallmark of sparse but salient content. It is calculated as:

$$\sigma_d = \sqrt{\frac{1}{L_d} \sum_{j=1}^{L_d} (I(\mathbf{d}_j) - \mu_d)^2}. \quad (4)$$

The adaptive pruning threshold τ_d for document d is then defined as a linear combination of these two statistics: $\tau_d = \mu_d + k \cdot \sigma_d$, where k is a hyperparameter that acts as a adaptation factor. It determines how many standard deviations above the mean a patch's importance score must be considered significant. We define the preliminary pruned set of patch embeddings $\hat{\mathbf{D}}'_d$ as:

$$\hat{\mathbf{D}}'_d = \{\mathbf{d}_j \in \mathbf{D}_d \mid I(\mathbf{d}_j) > \tau_d\}. \quad (5)$$

To handle the edge case where overly aggressive pruning might discard all embeddings (i.e., $\hat{\mathbf{D}}'_d = \emptyset$), we guarantee that at least one embedding is preserved. The final pruned set \mathbf{D}'_d is defined as:

$$\mathbf{D}'_d = \begin{cases} \hat{\mathbf{D}}'_d & \text{if } \hat{\mathbf{D}}'_d \neq \emptyset \\ \{\mathbf{d}_{j^*}\} \text{ where } j^* = \arg \max_{j \in \{1, \dots, L_d\}} I(\mathbf{d}_j) & \text{if } \hat{\mathbf{D}}'_d = \emptyset. \end{cases} \quad (6)$$

3.2.3 SCORING WITH PRUNED EMBEDDINGS

The ultimate goal of pruning is to reduce storage and, by extension, accelerate online retrieval, without compromising ranking quality. At query time, the retrieval process remains identical to the standard late-interaction paradigm, with one crucial difference: the search space for the MaxSim operation is significantly reduced. Instead of comparing each query token embedding against the full set of document embeddings \mathbf{D} , we use the compact, pruned set \mathbf{D}' . The pruned relevance score, $s'(q, d)$, is computed as: $s'(q, d) = \sum_{i=1}^{L_q} \max_{\mathbf{d}_j \in \mathbf{D}'} \mathbf{q}_i^\top \mathbf{d}_j$. For a given query q , we compute $s'(q, d_k)$ for all documents d_k in the corpus to obtain a ranked list. The effectiveness of this ranking is then evaluated using Normalized Discounted Cumulative Gain at rank 5 (nDCG@5).

3.3 THEORETICAL FOUNDATION

The efficacy of **DocPruner** can be rigorously analyzed through the **Information Bottleneck (IB) principle** (Tishby et al., 2000; Saxe et al., 2019; Tishby & Zaslavsky, 2015). The IB framework aims to learn a compressed representation \mathbf{Z} of an input random variable \mathbf{X} that is maximally informative about a target variable \mathbf{Y} . This is formulated as the following optimization problem:

$$\max_{\mathbf{Z}} \mathcal{L}_{IB}(\mathbf{Z}) = I(\mathbf{Z}; \mathbf{Y}) - \beta I(\mathbf{Z}; \mathbf{X}), \quad (7)$$

where $I(\cdot; \cdot)$ denotes mutual information and β is a Lagrangian multiplier balancing compression and information preservation.

The Intractable Ideal. In our VDR task, \mathbf{X} is the full set of document embeddings \mathbf{D} , \mathbf{Z} is the pruned set \mathbf{D}' , and the target \mathbf{Y} is the relevance score $s(q, d)$, which depends on a future, unknown query q . The ideal objective is to maximize the expected information about relevance over the distribution of all possible queries $P(q)$:

$$\max_{\mathbf{D}'} \mathbb{E}_{q \sim P(q)} [I(\mathbf{D}'; s(q, d))] \quad \text{s.t.} \quad |\mathbf{D}'| \ll |\mathbf{D}|. \quad (8)$$

This objective is intractable due to the unknown query distribution $P(q)$.

270 **DocPruner as a Tractable Approximation.** DocPruner offers a principled, tractable approximation to this problem.

271

- 272 ▶ **Global Token as Relevance Proxy.** The hidden state of global token, \mathbf{h}_{global} , serves as a sufficient
273 statistic for document’s relevance to an arbitrary query. That is, $I(\mathbf{D}; s(q, d)) \approx I(\mathbf{D}; \mathbf{h}_{global})$.
274 This axiom posits that the global token’s representation, which summarizes the entire document,
275 captures the necessary information for determining relevance. The attention scores $I(\mathbf{d}_j)$ directly
276 measure the information flow from each patch to this summary. Therefore, by selecting patches
277 that maximize $I(\mathbf{D}'; \mathbf{h}_{global})$, we are effectively approximating the ideal, intractable objective.
- 278 ▶ **Entropy-Aware Pruning.** The adaptive threshold τ_d dynamically adjusts the pruning ratio based
279 on the information entropy of the document’s attention distribution. Let the normalized attention
280 scores form a probability distribution $p_d(j) = \frac{I(\mathbf{d}_j)}{\sum_i I(\mathbf{d}_i)}$ over the patches. The information content
281 of the document is captured by its Shannon entropy $H(p_d) = -\sum_j p_d(j) \log p_d(j)$.

282

- 283 1. **Low-Entropy Documents:** For documents with low information entropy (e.g., title pages),
284 p_d is a sparse, peaky distribution. A few patches have very high attention scores, while most
285 have near-zero scores. The term $k \cdot \sigma_d$ dominates, setting a high threshold τ_d that isolates
286 only the highly informative “outlier” patches, resulting in aggressive pruning.
- 287 2. **High-Entropy Documents:** For documents with high information entropy (e.g., dense
288 text pages), p_d is more uniform. Attention scores are distributed more evenly across many
289 patches. The threshold τ_d is more lenient, preserving a larger patch number that collectively
290 contribute to the document’s meaning.

291 4 EXPERIMENT

292 4.1 EXPERIMENTAL SETUP

293 **Benchmarks & Evaluation.** We conduct our experiments on recent representative VDR benchmarks:
294 **ViDoRe-V2** (Macé et al., 2025) and **JinaVDR-Bench** (Günther et al., 2025) (More details in Appendix C). We use three state-of-the-art multi-vector VDR models as our base models:
295 **ColQwen2.5** (Faysse et al., 2024), **ColNomic** (NomicAI, 2025), and **Jina Embeddings V4**
296 (Günther et al., 2025). Following standard practice in VDR domain (Faysse et al., 2024; Günther
297 et al., 2025; NomicAI, 2025; Xu et al., 2025a), we use **nDCG@5** as the primary evaluation metric.

300 **Baselines.** We compare DocPruner against three categories of baselines.

301 (I) **Base Models.** This represents the original multi-vector models without any pruning or merging.
302 They serve as the performance upper bound of storage cost.

303 (II) **Merging-based Methods.** Following Ma et al. (2025), the only work focused on VDR storage
304 optimization via merging, we implement three merging strategies:

305

- 306 ▶ **Sem-Cluster:** Merges patch embeddings by performing hierarchical clustering and representing
307 each cluster by its centroid. The tunable hyperparameter is the `merging_factor`, which
308 determines the target number of clusters.
- 309 ▶ **1D-Pooling:** Applies 1D average pooling over sequential groups of patch embeddings to reduce
310 their count. The hyperparameter is `merging_factor`, which defines the pooling window size.
- 311 ▶ **2D-Pooling:** Arranges patch embeddings into a 2D grid and applies 2D average pooling. The
312 hyperparameter is `merging_factor`, which must be a perfect square.

313 (III) **Pruning-based Methods:** We compare three pruning strategies adapted to VDR context:

314

- 315 ▶ **Random:** Randomly discards a fixed fraction of patch embeddings, serving as a naive baseline.
316 The hyperparameter is the `pruning_ratio`.
- 317 ▶ **Attention-plus-Similarity:** An adaptive method that computes a combined score from both the
318 [EOS] attention (importance) and the embedding similarity to the [EOS] token (representativeness),
319 then prunes patches below a dynamically calculated threshold, following Wen et al. (2025).
320 Hyperparameters include an adaptive factor `k` and a weighting factor `alpha`.
- 321 ▶ **Pivot-Threshold:** A two-stage adaptive method that first filters an “important set” of patches
322 using an adaptive attention threshold, and then de-duplicates this set by pruning patches that
323 are too similar to selected “pivot”, following VisPruner (Zhang et al., 2025c). Hyperparameters
324 include an adaptive factor for importance `k`, a de-duplication factor `k_dup`, and `num_pivots`.

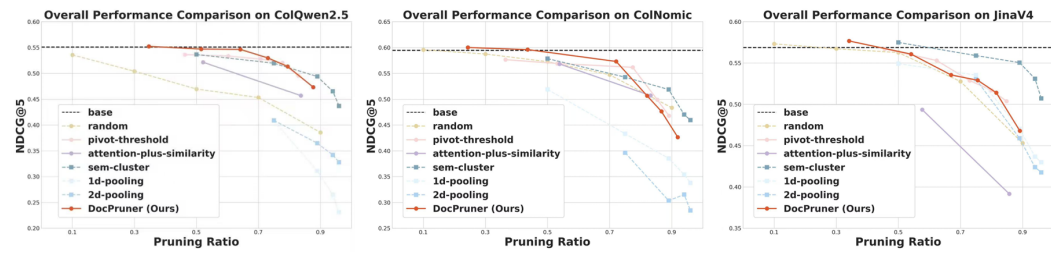


Figure 2: Performance comparison (nDCG@5) between DocPruner and baselines on ViDoRe-V2 benchmark (Macé et al., 2025) across ColQwen2.5 (*Left*), ColNomic (*Middle*), and Jina Embedding V4 (*Right*). Here, *solid lines* denote adaptive methods, whereas *dashed lines* denote non-adaptive ones; *circular nodes* represent pruning methods, whereas *square nodes* represent merging methods.

Implementation Details. To ensure fair and reproducible comparisons, we replicated the base results of three base models in aligned with their respective official implementation. Our evaluation codebase is adapted from the official ViDoRe Benchmark repository¹. The complete code for our experiments, including all baseline implementations and the DocPruner framework, will be made publicly available upon acceptance. For DocPruner, the adaptation factor k has a range of $\{-0.5, -0.25, 0, 0.25, 0.5, 1\}$. The details of hyperparameters for all baseline methods is detailed in the Appendix D. All experiments were conducted on a NVIDIA A100 (80GB) GPU cluster.

4.2 EXPERIMENTAL ANALYSIS

In this section, we conduct a comprehensive experimental analysis to answer four key research questions (RQs). **(RQ1)** How effectively does DocPruner maintain retrieval performance on diverse visual document types while achieving significant storage compression? **(RQ2)** Can DocPruner’s robust performance generalize to multilingual retrieval scenarios? **(RQ3)** What is the difference between DocPruner framework and its variants? **(RQ4)** What are the quantifiable relative improvements in storage efficiency and latency of implementing DocPruner?

4.2.1 RETRIEVAL PERFORMANCE COMPARISON (RQ1)

To answer RQ1, we evaluate DocPruner’s performance against a comprehensive set of baselines on the ViDoRe-V2 benchmark. The results, visualized in Figure 2, demonstrate the effectiveness and robustness of our approach across three leading multi-vector models. See more results in Sec. E.1.

Observation 1: DocPruner achieves near-lossless retrieval performance while pruning 50-60% of embeddings, demonstrating remarkable robustness across different base models. As illustrated in Figure 2, DocPruner consistently operates near the performance ceiling set by the unpruned base models (*i.e.*, dashed black line) even when around 60% of embeddings are pruned. For instance, when applied to ColQwen2.5, DocPruner removes 51.6% of patch embeddings with a mere 0.0038 drop in nDCG@5 (from 0.5508 to 0.5470). This high efficiency is mirrored on Jina Embedding V4, where it prunes 54.1% of embeddings while the nDCG@5 only decreases from 0.5687 to 0.5608. Even on the high-performing ColNomic model, DocPruner achieves a 43.6% pruning ratio with a negligible performance change (0.5960 vs. the base’s 0.5946), showcasing a remarkable balance between efficiency and accuracy. This robustness stems from DocPruner’s mechanism, which leverages intra-document attention to create a document-specific importance score for each patch, effectively retaining the most semantically salient information necessary for retrieval.

Observation 2: Pruning-based strategies are generally more effective at preserving retrieval performance than merging-based strategies. This trend is evident across all three models, where methods marked with circles (pruning) consistently form a higher-performance frontier than those with squares (merging). For instance, on the ColNomic model at a around 75% compression ratio, DocPruner achieves an nDCG@5 of 0.5730 (at a 72.1% ratio), whereas the strongest merging baseline, sem-cluster, drops to 0.5426 (at a 75% ratio). The reason for this disparity is that merging, by averaging feature vectors, can dilute the distinctiveness of highly salient patches, blurring important signals. In contrast, pruning preserves the original, high-fidelity embeddings of the most critical patches, vital for the late-interaction mechanism’s ability to find precise query-patch matches.

¹<https://github.com/illuin-tech/vidore-benchmark>

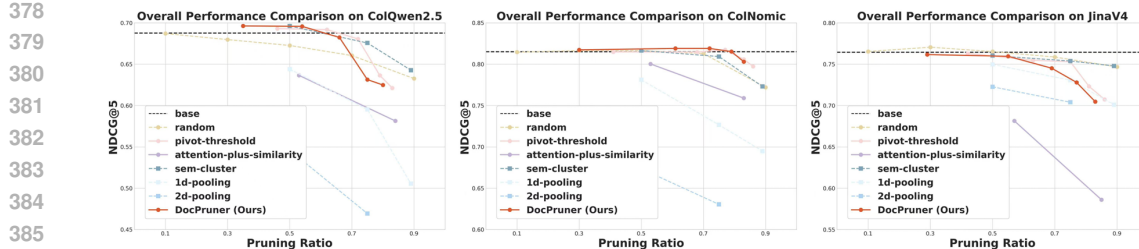


Figure 4: Performance comparison (nDCG@5) between DocPruner and baselines on JinaVDR benchmark (Günther et al., 2025) across ColQwen2.5 (**Left**), ColNomic (**Middle**), and Jina Embedding V4 (**Right**). Here, *solid lines* denote adaptive methods, whereas *dashed lines* denote non-adaptive ones; *circular nodes* represent pruning methods, whereas *square nodes* represent merging methods.

Observation ③: Adaptive pruning methods generally exhibit a superior performance-compression trade-off compared to non-adaptive, fixed-ratio approaches. The solid lines in Figure 2, representing adaptive methods like DocPruner, consistently maintain higher nDCG@5 scores than their non-adaptive counterparts (dashed lines) at similar compression levels (esp., below 60% ratio). For example, on the ColNomic model, DocPruner achieves a high nDCG@5 of 0.5960 with a 43.6% pruning ratio, outperforming all non-adaptive baselines. The superiority of adaptive methods is because they intelligently account for the heterogeneity of visual documents (validated by Figure 3); they prune more aggressively on information-sparse pages and more conservatively on information-dense ones, whereas fixed-ratio methods apply a one-size-fits-all strategy that can be suboptimal.

Observation ④: Notably, merging-based methods exhibit uncharacteristically strong performance on the Jina Embedding V4, in some cases surpassing DocPruner. This phenomenon can likely be attributed to JinaV4’s unique training architecture; its technical report (Günther et al., 2025) reveals that the model is explicitly co-trained to produce a single-vector embedding via mean_pooling over its token-level representations. This training paradigm encourages the model to learn patch embeddings that are inherently more aggregable and robust to averaging, making post-hoc merging strategies unusually effective as they align with the model’s intrinsic properties.

4.2.2 GENERALIZATION TO MULTILINGUAL SCENARIOS (RQ2)

To answer RQ2, we evaluate DocPruner’s generalization capability on the multilingual JinaVDR benchmark, where we choose documents in German, Russian, Chinese, and Japanese. The overall and per-language results, presented in Figure 4 and Sec.E.2, lead to the following observations.

Observation ⑤: DocPruner demonstrates strong and consistent performance across diverse multilingual datasets, maintaining near-lossless retrieval accuracy while achieving substantial storage savings (i.e., around 50-60%). For instance, on the ColNomic model, DocPruner achieves a remarkable 61.0% overall pruning ratio with a slight increase in nDCG@5 from the base’s 0.8151 to 0.8191. Similarly, when applied to ColQwen2.5, it prunes 54.0% of embeddings while improving the nDCG@5 score from 0.6877 to 0.6958. This robust generalization stems from DocPruner’s core mechanism, which relies on the *language-agnostic* visual attention patterns within the VLM.

Observation ⑥: DocPruner’s adaptive nature is particularly evident in its ability to dynamically adjust pruning ratios for documents in different languages, reflecting varying information densities. This tailored approach is clearly visible in the per-language pruning statistics shown in Appendix E.2. Using the ColNomic model as an example (with $k=-0.5$), DocPruner applies a modest pruning ratio of 9.0% for German documents (nDCG@5 of 0.6022 vs. base 0.5975) and 7.0% for Spanish documents (nDCG@5 of 0.7896 vs. base 0.7927). In contrast, it identifies greater redundancy in other languages, pruning 36.3% for Japanese and 37.6% for Chinese documents while maintaining high performance. This demonstrates that DocPruner is not applying a uniform rule

432 but is sensitive to the intrinsic properties of the documents themselves, automatically allocating the
 433 storage budget proportional to each document’s information entropy.
 434

435 4.2.3 VARIANT STUDY (RQ3) 436

437 To answer RQ3, we conduct a variant study comparing **DocPruner** against pruning-based variants
 438 (shown in Figure 5), which are: **(I) attention-ratio**, a non-adaptive method that prunes a fixed
 439 percentage of patches with the lowest attention scores; **(II) attention-threshold**, which uses a fixed,
 440 global attention value as the pruning threshold; and **(III) attention-threshold-nfp**, which enhances
 441 the static threshold method with a noise-filtering-prompt (nfp) to guide the model’s focus.

442 **Observation ⑦: The document-adaptive**
 443 **statistical thresholding of DocPruner consistently achieves a superior performance-**
 444 **compression trade-off compared to simpler**
 445 **pruning variants that rely on fixed ratios or**
 446 **static thresholds.** While all methods leverage
 447 attention scores, their pruning criteria differ fundamentally: attention-ratio enforces a
 448 uniform compression rate, whereas attention-threshold and attention-threshold-nfp apply a
 449 one-size-fits-all importance cutoff. At a significant pruning ratio of approximately 60%,
 450 **DocPruner** sustains a high nDCG@5 of 0.54;
 451 but the performance of the static attention-
 452 threshold variant collapses to below 0.45, and
 453 even the improved attention-threshold-nfp and fixed-ratio attention-ratio methods lag considerably.
 454

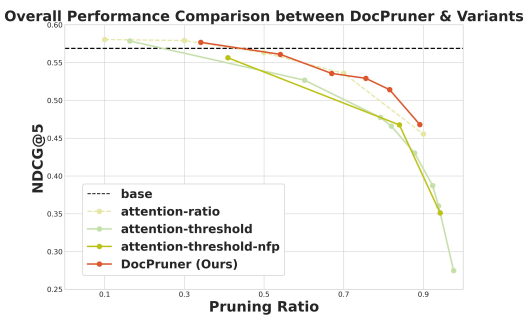
455 4.2.4 EFFICIENCY ANALYSIS (RQ4) 456

457 **Observation ⑧: DocPruner achieves a substantial**
 458 **storage footprint reduction of approximately**
 459 **50% on average with near-lossless retrieval per-**
 460 **formance, at the cost of an acceptable increase**
 461 **in offline encoding latency.** As detailed in Ta-
 462 **ble 1**, **DocPruner** reduces storage footprints by
 463 51.55% for ColQwen, 43.62% for ColNomic, and
 464 54.09% for JinaV4, while the nDCG@5 per-
 465 formance changes are minimal (\downarrow 0.69%, \uparrow 0.24%, and
 466 \downarrow 1.39%, respectively). This specific setting of $k=-0.25$ consistently delivers an optimal trade-off be-
 467 between performance and storage across all multi-vector models. Although **DocPruner** introduces an
 468 overhead that increases offline latency by 60-66% due to the extra steps of attention score extraction
 469 and filtering, the practical impact is modest. The average per-document encoding time increases
 470 from a baseline of 0.47s to only 0.77s, a duration that is acceptable for an offline indexing phase and
 471 vastly superior to 7.22s required by OCR-based method (*i.e.*, OCR+BGE-M3 (Chen et al., 2024a)).
 472

473 5 CONCLUSION 474

475 In this paper, we addressed the critical challenge of prohibitive storage overhead in state-of-the-art
 476 multi-vector VDR systems. We introduced **DocPruner**, a novel and adaptive framework for patch-
 477 level embedding pruning, which leverages the attention paid by a global token to each image patch
 478 to derive a query-agnostic importance score. Crucially, **DocPruner** employs a document-specific
 479 statistical threshold, allowing it to dynamically adjust the pruning ratio for documents of varying
 480 information density and complexity. Through extensive experiments across more than ten bench-
 481 mark datasets, we have demonstrated that **DocPruner** can achieve a substantial 50-60% reduction in
 482 stored patch embeddings with only negligible degradation in retrieval accuracy. Future work could
 483 explore integrating this pruning mechanism directly into the model training process or extending
 484 the adaptive principle to other modalities. Ultimately, **DocPruner** charts a path toward fine-grained
 485 multimodal understanding as practical, real-world applications at an unprecedented scale.

486 We elaborate the broader impact of **DocPruner** and LLM usage in Section F and G, respectively.



487 **Figure 5:** Overall comparison between **DocPruner** &
 488 variants (See per-dataset analysis in Sec.E.3).

489 **Table 1:** Relative improvement of **performance**,
 490 **storage**, and **latency** to base models on ViDoRe-
 491 V2 (adaptation factor k as -0.25; **orange** denotes
 492 better and **green** denotes worse).

Δ	ColQwen	ColNomic	JinaV4
nDCG@5	\downarrow 0.69%	\uparrow 0.24%	\downarrow 1.39%
Storage	\downarrow 51.55%	\downarrow 43.62%	\downarrow 54.09%
Latency	\uparrow 60.00%	\uparrow 65.96%	\uparrow 66.00%

493 This specific setting of $k=-0.25$ consistently delivers an optimal trade-off be-
 494 between performance and storage across all multi-vector models. Although **DocPruner** introduces an
 495 overhead that increases offline latency by 60-66% due to the extra steps of attention score extraction
 496 and filtering, the practical impact is modest. The average per-document encoding time increases
 497 from a baseline of 0.47s to only 0.77s, a duration that is acceptable for an offline indexing phase and
 498 vastly superior to 7.22s required by OCR-based method (*i.e.*, OCR+BGE-M3 (Chen et al., 2024a)).
 499

486 REFERENCES
487

488 Mohammad Mahdi Abootorabi, Amirhosein Zobeiri, Mahdi Dehghani, Mohammadali Mohammad-
489 khani, Bardia Mohammadi, Omid Ghahroodi, Mahdieh Soleymani Baghshah, and Ehsaneddin
490 Asgari. Ask in any modality: A comprehensive survey on multimodal retrieval-augmented gen-
491 eration. *arXiv preprint arXiv:2502.08826*, 2025.

492 Antonio Acquavia, Craig Macdonald, and Nicola Tonelotto. Static pruning for multi-representation
493 dense retrieval. In *Proceedings of the ACM Symposium on Document Engineering 2023*, pp. 1–10,
494 2023.

495 Shuai Bai, Keqin Chen, Xuejing Liu, Jialin Wang, Wenbin Ge, Sibo Song, Kai Dang, Peng Wang,
496 Shijie Wang, Jun Tang, et al. Qwen2. 5-vl technical report. *arXiv preprint arXiv:2502.13923*,
497 2025.

498 Zechen Bai, Pichao Wang, Tianjun Xiao, Tong He, Zongbo Han, Zheng Zhang, and Mike Zheng
499 Shou. Hallucination of multimodal large language models: A survey. *arXiv preprint arXiv:2404.18930*,
500 2024.

501 Lucas Beyer, Andreas Steiner, André Susano Pinto, Alexander Kolesnikov, Xiao Wang, Daniel Salz,
502 Maxim Neumann, Ibrahim Alabdulmohsin, Michael Tschannen, Emanuele Bugliarello, et al.
503 Paligemma: A versatile 3b vlm for transfer. *arXiv preprint arXiv:2407.07726*, 2024.

504 Zheng Bian, Man Lung Yiu, and Bo Tang. Igp: Efficient multi-vector retrieval via proximity graph
505 index. In *Proceedings of the 48th International ACM SIGIR Conference on Research and Devel-
506 opment in Information Retrieval*, pp. 2524–2533, 2025.

507 Daniel Bolya, Cheng-Yang Fu, Xiaoliang Dai, Peizhao Zhang, Christoph Feichtenhofer, and Judy
508 Hoffman. Token merging: Your vit but faster. *arXiv preprint arXiv:2210.09461*, 2022.

509 Ekaterina Borisova, Nikolas Rauscher, and Georg Rehm. Scivqa 2025: Overview of the first sci-
510 entific visual question answering shared task. In *Proceedings of the Fifth Workshop on Scholarly
511 Document Processing (SDP 2025)*, pp. 182–210, 2025.

512 Davide Caffagni, Federico Cocchi, Luca Barsellotti, Nicholas Moratelli, Sara Sarto, Lorenzo
513 Baraldi, Marcella Cornia, and Rita Cucchiara. The revolution of multimodal large language mod-
514 els: a survey. *arXiv preprint arXiv:2402.12451*, 2024.

515 Jianlv Chen, Shitao Xiao, Peitian Zhang, Kun Luo, Defu Lian, and Zheng Liu. Bge m3-embedding:
516 Multi-lingual, multi-functionality, multi-granularity text embeddings through self-knowledge dis-
517 tillation. *arXiv preprint arXiv:2402.03216*, 2024a.

518 Junkai Chen, Zhijie Deng, Kening Zheng, Yibo Yan, Shuliang Liu, PeiJun Wu, Peijie Jiang, Jia Liu,
519 and Xuming Hu. Safeeraser: Enhancing safety in multimodal large language models through
520 multimodal machine unlearning. *arXiv preprint arXiv:2502.12520*, 2025.

521 Liang Chen, Haozhe Zhao, Tianyu Liu, Shuai Bai, Junyang Lin, Chang Zhou, and Baobao Chang.
522 An image is worth 1/2 tokens after layer 2: Plug-and-play inference acceleration for large vision-
523 language models. In *European Conference on Computer Vision*, pp. 19–35. Springer, 2024b.

524 Hongrong Cheng, Miao Zhang, and Javen Qinfeng Shi. A survey on deep neural network pruning:
525 Taxonomy, comparison, analysis, and recommendations. *IEEE Transactions on Pattern Analysis
526 and Machine Intelligence*, 2024a.

527 Xin Cheng, Xun Wang, Xingxing Zhang, Tao Ge, Si-Qing Chen, Furu Wei, Huishuai Zhang, and
528 Dongyan Zhao. xrag: Extreme context compression for retrieval-augmented generation with one
529 token. *Advances in Neural Information Processing Systems*, 37:109487–109516, 2024b.

530 Benjamin Clavić, Antoine Chaffin, and Griffin Adams. Reducing the footprint of multi-vector re-
531 trieval with minimal performance impact via token pooling. *arXiv preprint arXiv:2409.14683*,
532 2024.

533 Yihao Ding, Soyeon Caren Han, Jean Lee, and Eduard Hovy. Deep learning based visually rich
534 document content understanding: A survey. *arXiv preprint arXiv:2408.01287*, 2024.

540 Kucai Dong, Yujing Chang, Xin Deik Goh, Dexun Li, Ruiming Tang, and Yong Liu. Mmdocir:
 541 Benchmarking multi-modal retrieval for long documents. *arXiv preprint arXiv:2501.08828*, 2025.
 542

543 Zane Durante, Qiuyuan Huang, Naoki Wake, Ran Gong, Jae Sung Park, Bidipta Sarkar, Rohan
 544 Taori, Yusuke Noda, Demetri Terzopoulos, Yejin Choi, et al. Agent ai: Surveying the horizons of
 545 multimodal interaction. *arXiv preprint arXiv:2401.03568*, 2024.

546 Junfeng Fang, Yukai Wang, Ruipeng Wang, Zijun Yao, Kun Wang, An Zhang, Xiang Wang, and
 547 Tat-Seng Chua. Safemrlm: Demystifying safety in multi-modal large reasoning models. *arXiv
 548 preprint arXiv:2504.08813*, 2025.

549

550 Manuel Faysse, Hugues Sibille, Tony Wu, Bilel Omrani, Gautier Viaud, Céline Hudelot, and Pierre
 551 Colombo. Colpali: Efficient document retrieval with vision language models. *arXiv preprint
 552 arXiv:2407.01449*, 2024.

553

554 Marco Federici, Davide Belli, Mart Van Baalen, Amir Jalalirad, Andrii Skliar, Bence Major, Markus
 555 Nagel, and Paul Whatmough. Efficient llm inference using dynamic input pruning and cache-
 556 aware masking. *arXiv preprint arXiv:2412.01380*, 2024.

557

558 Aaron Grattafiori, Abhimanyu Dubey, Abhinav Jauhri, Abhinav Pandey, Abhishek Kadian, Ahmad
 559 Al-Dahle, Aiesha Letman, Akhil Mathur, Alan Schelten, Alex Vaughan, et al. The llama 3 herd
 560 of models. *arXiv preprint arXiv:2407.21783*, 2024.

561

562 Michael Günther, Saba Sturua, Mohammad Kalim Akram, Isabelle Mohr, Andrei Ungureanu,
 563 Bo Wang, Sedigheh Eslami, Scott Martens, Maximilian Werk, Nan Wang, et al. jina-
 564 embeddings-v4: Universal embeddings for multimodal multilingual retrieval. *arXiv preprint
 565 arXiv:2506.18902*, 2025.

566

567 Hao Guo, Xugong Qin, Jun Jie Ou Yang, Peng Zhang, Gangyan Zeng, Yubo Li, and Hailun Lin.
 568 Towards natural language-based document image retrieval: New dataset and benchmark. In *Pro-
 ceedings of the Computer Vision and Pattern Recognition Conference*, pp. 29722–29732, 2025.

569

570 Thomas Hegghammer. Ocr with tesseract, amazon textract, and google document ai: a benchmark-
 571 ing experiment. *Journal of Computational Social Science*, 5(1):861–882, 2022.

572

573 Bairu Hou, Qibin Chen, Jianyu Wang, Guoli Yin, Chong Wang, Nan Du, Ruoming Pang, Shiyu
 574 Chang, and Tao Lei. Instruction-following pruning for large language models. *arXiv preprint
 575 arXiv:2501.02086*, 2025a.

576

577 Ce Hou, Fan Zhang, Yong Li, Haifeng Li, Gengchen Mai, Yuhao Kang, Ling Yao, Wenhao Yu, Yao
 578 Yao, Song Gao, et al. Urban sensing in the era of large language models. *The Innovation*, 6(1),
 579 2025b.

580

581 Anwen Hu, Haiyang Xu, Jiabo Ye, Ming Yan, Liang Zhang, Bo Zhang, Chen Li, Ji Zhang, Qin Jin,
 582 Fei Huang, et al. mplug-docowl 1.5: Unified structure learning for ocr-free document understand-
 583 ing. *arXiv preprint arXiv:2403.12895*, 2024a.

584

585 Anwen Hu, Haiyang Xu, Liang Zhang, Jiabo Ye, Ming Yan, Ji Zhang, Qin Jin, Fei Huang, and
 586 Jingren Zhou. mplug-docowl2: High-resolution compressing for ocr-free multi-page document
 587 understanding. *arXiv preprint arXiv:2409.03420*, 2024b.

588

589 Haoming Huang, Yibo Yan, Jiahao Huo, Xin Zou, Xinfeng Li, Kun Wang, and Xuming Hu. Pierce
 590 the mists, greet the sky: Decipher knowledge overshadowing via knowledge circuit analysis.
 591 *arXiv preprint arXiv:2505.14406*, 2025.

592

593 Kai Huang, Hao Zou, Ye Xi, BoChen Wang, Zhen Xie, and Liang Yu. Ivtp: Instruction-guided
 594 visual token pruning for large vision-language models. In *European Conference on Computer
 595 Vision*, pp. 214–230. Springer, 2024.

596

597 Jiahao Huo, Yibo Yan, Boren Hu, Yutao Yue, and Xuming Hu. Mmneuron: Discovering
 598 neuron-level domain-specific interpretation in multimodal large language model. *arXiv preprint
 599 arXiv:2406.11193*, 2024.

594 Jiahao Huo, Yibo Yan, Xu Zheng, Yuanhuiyi Lyu, Xin Zou, Zhihua Wei, and Xuming Hu.
 595 Mmlearner: Reformulating multimodal machine unlearning in the era of multimodal large lan-
 596 guage models. *arXiv preprint arXiv:2502.11051*, 2025.

597 Youngrok Jang, Hyesoo Kong, Gyeonghun Kim, Yejin Lee, Jungkyu Choi, and Kyunghoon Bae. Ict-
 598 qa: Question answering over multi-modal contexts including image, chart, and text modalities. In
 599 *Proceedings of the Computer Vision and Pattern Recognition Conference*, pp. 138–148, 2025.

600 Rajesh Jayaram, Laxman Dhulipala, Majid Hadian, Jason D Lee, and Vahab Mirrokni. Muvera:
 601 Multi-vector retrieval via fixed dimensional encoding. *Advances in Neural Information Process-
 602 ing Systems*, 37:101042–101073, 2024.

603 Ziwei Ji, Himanshu Jain, Andreas Veit, Sashank J Reddi, Sadeep Jayasumana, Ankit Singh Rawat,
 604 Aditya Krishna Menon, Felix Yu, and Sanjiv Kumar. Efficient document ranking with learnable
 605 late interactions. *arXiv preprint arXiv:2406.17968*, 2024.

606 Lei Jiang, Weizhe Huang, Tongxuan Liu, Yuting Zeng, Jing Li, Lechao Cheng, and Xiaohua Xu. Fop-
 607 pru: Focal pruning for efficient large vision-language models. *arXiv preprint arXiv:2411.14164*,
 608 2024a.

609 Ziyang Jiang, Rui Meng, Xinyi Yang, Semih Yavuz, Yingbo Zhou, and Wenhui Chen. Vlm2vec:
 610 Training vision-language models for massive multimodal embedding tasks. *arXiv preprint
 611 arXiv:2410.05160*, 2024b.

612 Tomoyuki Kagaya, Thong Jing Yuan, Yuxuan Lou, Jayashree Karlekar, Sugiri Pranata, Akira Ki-
 613 nose, Koki Oguri, Felix Wick, and Yang You. Rap: Retrieval-augmented planning with contextual
 614 memory for multimodal llm agents. *arXiv preprint arXiv:2402.03610*, 2024.

615 Leonid Karlinsky, Assaf Arbelle, Abraham Daniels, Ahmed Nassar, Amit Alfassi, Bo Wu, Eli
 616 Schwartz, Dhiraj Joshi, Jovana Kondic, et al. Granite vision: a lightweight, open-source multi-
 617 modal model for enterprise intelligence. *arXiv preprint arXiv:2502.09927*, 2025.

618 Vladimir Karpukhin, Barlas Oguz, Sewon Min, Patrick SH Lewis, Ledell Wu, Sergey Edunov, Danqi
 619 Chen, and Wen-tau Yih. Dense passage retrieval for open-domain question answering. In *EMNLP
 620 (1)*, pp. 6769–6781, 2020.

621 Omar Khattab and Matei Zaharia. Colbert: Efficient and effective passage search via contextualized
 622 late interaction over bert. In *Proceedings of the 43rd International ACM SIGIR conference on
 623 research and development in Information Retrieval*, pp. 39–48, 2020.

624 Carlos Lassance, Simon Lupart, Hervé Déjean, Stéphane Clinchant, and Nicola Tonellootto. A static
 625 pruning study on sparse neural retrievers. In *Proceedings of the 46th International ACM SIGIR
 626 Conference on Research and Development in Information Retrieval*, pp. 1771–1775, 2023.

627 Jinhyuk Lee, Zhuyun Dai, Sai Meher Karthik Duddu, Tao Lei, Iftekhar Naim, Ming-Wei Chang,
 628 and Vincent Zhao. Rethinking the role of token retrieval in multi-vector retrieval. *Advances in
 629 Neural Information Processing Systems*, 36:15384–15405, 2023.

630 Bo Li, Yuanhan Zhang, Dong Guo, Renrui Zhang, Feng Li, Hao Zhang, Kaichen Zhang, Peiyuan
 631 Zhang, Yanwei Li, Ziwei Liu, et al. Llava-onevision: Easy visual task transfer. *arXiv preprint
 632 arXiv:2408.03326*, 2024a.

633 Feng Li, Renrui Zhang, Hao Zhang, Yuanhan Zhang, Bo Li, Wei Li, Zejun Ma, and Chunyuan Li.
 634 Llava-next-interleave: Tackling multi-image, video, and 3d in large multimodal models. *arXiv
 635 preprint arXiv:2407.07895*, 2024b.

636 Junnan Li, Dongxu Li, Silvio Savarese, and Steven Hoi. Blip-2: Bootstrapping language-image
 637 pre-training with frozen image encoders and large language models. In *International conference
 638 on machine learning*, pp. 19730–19742. PMLR, 2023.

639 Xin Li, Yunfei Wu, Xinghua Jiang, Zhihao Guo, Mingming Gong, Haoyu Cao, Yinsong Liu, De-
 640 qiang Jiang, and Xing Sun. Enhancing visual document understanding with contrastive learning in
 641 large visual-language models. In *Proceedings of the IEEE/CVF Conference on Computer Vision
 642 and Pattern Recognition*, pp. 15546–15555, 2024c.

648 Sheng-Chieh Lin, Chankyu Lee, Mohammad Shoeybi, Jimmy Lin, Bryan Catanzaro, and Wei
 649 Ping. Mm-embed: Universal multimodal retrieval with multimodal llms. *arXiv preprint*
 650 *arXiv:2411.02571*, 2024.

651

652 Zihao Lin, Samyadeep Basu, Mohammad Beigi, Varun Manjunatha, Ryan A Rossi, Zichao Wang,
 653 Yufan Zhou, Sriram Balasubramanian, Arman Zarei, Keivan Rezaei, et al. A survey on mechanis-
 654 tic interpretability for multi-modal foundation models. *arXiv preprint arXiv:2502.17516*, 2025.

655 Junyi Liu, Liangzhi Li, Tong Xiang, Bowen Wang, and Yiming Qian. Tcra-llm: Token com-
 656 pression retrieval augmented large language model for inference cost reduction. *arXiv preprint*
 657 *arXiv:2310.15556*, 2023.

658

659 Qi Liu, Gang Guo, Jiaxin Mao, Zhicheng Dou, Ji-Rong Wen, Hao Jiang, Xinyu Zhang, and Zhao
 660 Cao. An analysis on matching mechanisms and token pruning for late-interaction models. *ACM*
 661 *Transactions on Information Systems*, 42(5):1–28, 2024.

662 Shuliang Liu, Qi Zheng, Jesse Jiaxi Xu, Yibo Yan, He Geng, Aiwei Liu, Peijie Jiang, Jia Liu, Yik-
 663 Cheung Tam, and Xuming Hu. Vla-mark: A cross modal watermark for large vision-language
 664 alignment model. *arXiv preprint arXiv:2507.14067*, 2025a.

665

666 Ze Liu, Zhengyang Liang, Junjie Zhou, Zheng Liu, and Defu Lian. Any information is just worth
 667 one single screenshot: Unifying search with visualized information retrieval. *arXiv preprint*
 668 *arXiv:2502.11431*, 2025b.

669

670 Yihao Lu and Hao Tang. Multimodal data storage and retrieval for embodied ai: A survey. *arXiv*
 671 *preprint arXiv:2508.13901*, 2025.

672

673 Xueguang Ma, Sheng-Chieh Lin, Minghan Li, Wenhui Chen, and Jimmy Lin. Unifying multimodal
 674 retrieval via document screenshot embedding. *arXiv preprint arXiv:2406.11251*, 2024.

675

676 Yubo Ma, Jinsong Li, Yuhang Zang, Xiaobao Wu, Xiaoyi Dong, Pan Zhang, Yuhang Cao, Haodong
 677 Duan, Jiaqi Wang, Yixin Cao, et al. Towards storage-efficient visual document retrieval: An
 678 empirical study on reducing patch-level embeddings. *arXiv preprint arXiv:2506.04997*, 2025.

679

680 Sean MacAvaney, Antonio Mallia, and Nicola Tonellotto. Efficient constant-space multi-vector
 681 retrieval. In *European Conference on Information Retrieval*, pp. 237–245. Springer, 2025.

682

683 Quentin Macé, António Loison, and Manuel Faysse. Vidore benchmark v2: Raising the bar for
 684 visual retrieval, 2025. URL <https://arxiv.org/abs/2505.17166>.

685

686 Yuren Mao, Xuemei Dong, Wenyi Xu, Yunjun Gao, Bin Wei, and Ying Zhang. Fit-rag: Black-box
 687 rag with factual information and token reduction. *ACM Transactions on Information Systems*, 43
 688 (2):1–27, 2025.

689

690 Lang Mei, Siyu Mo, Zhihan Yang, and Chong Chen. A survey of multimodal retrieval-augmented
 691 generation. *arXiv preprint arXiv:2504.08748*, 2025.

692

693 Rui Meng, Ziyan Jiang, Ye Liu, Mingyi Su, Xinyi Yang, Yuepeng Fu, Can Qin, Zeyuan Chen, Ran
 694 Xu, Caiming Xiong, et al. Vlm2vec-v2: Advancing multimodal embedding for videos, images,
 695 and visual documents. *arXiv preprint arXiv:2507.04590*, 2025.

696

697 Alexander Most, Joseph Winjum, Manish Bhattacharai, Shawn Jones, Nishath Rajiv Ranasinghe, Ayan
 698 Biswas, and Dan O’Malley. Lost in ocr translation? vision-based approaches to robust document
 699 retrieval. In *Proceedings of the 2025 ACM Symposium on Document Engineering*, pp. 1–10, 2025.

700

701 NomicAI. Nomic embed multimodal: Interleaved text, image, and screenshots for
 702 visual document retrieval, 2025. URL <https://nomic.ai/blog/posts/nomic-embed-multimodal>.

703

704 Cheoneum Park, Seohyeong Jeong, Minsang Kim, KyungTae Lim, and Yong-Hun Lee. Scv: Light
 705 and effective multi-vector retrieval with sequence compressive vectors. In *Proceedings of the 31st*
 706 *International Conference on Computational Linguistics: Industry Track*, pp. 760–770, 2025.

702 Beth Plale, Sai Navya Jyesta, and Sachith Withana. Vector embedding of multi-modal texts: a tool
 703 for discovery? *arXiv preprint arXiv:2509.08216*, 2025.

704

705 Keshav Santhanam, Omar Khattab, Jon Saad-Falcon, Christopher Potts, and Matei Zaharia.
 706 Colbertv2: Effective and efficient retrieval via lightweight late interaction. *arXiv preprint*
 707 *arXiv:2112.01488*, 2021.

708

709 Keshav Santhanam, Omar Khattab, Christopher Potts, and Matei Zaharia. Plaid: an efficient en-
 710 gine for late interaction retrieval. In *Proceedings of the 31st ACM International Conference on*
 711 *Information & Knowledge Management*, pp. 1747–1756, 2022.

712

713 Andrew M Saxe, Yamini Bansal, Joel Dapello, Madhu Advani, Artemy Kolchinsky, Brendan D
 714 Tracey, and David D Cox. On the information bottleneck theory of deep learning. *Journal of*
 715 *Statistical Mechanics: Theory and Experiment*, 2019(12):124020, 2019.

716

717 Jan Luca Scheerer, Matei Zaharia, Christopher Potts, Gustavo Alonso, and Omar Khattab. Warp: An
 718 efficient engine for multi-vector retrieval. In *Proceedings of the 48th International ACM SIGIR*
 719 *Conference on Research and Development in Information Retrieval*, pp. 2504–2512, 2025.

720

721 Shanghai Municipal People’s Government Urban Planning and Land Resource Administration
 722 Bureau. *Shanghai Master Plan 2017–2035: Striving for the Excellent Global City*. Shanghai
 723 Municipal People’s Government, Shanghai, China, January 2018. URL <https://www.shanghai.gov.cn/newshanghai/xxgk/j/2035004.pdf>. Public Reading edition;
 724 government-issued planning document.

725

726 Susav Shrestha, Narasimha Reddy, and Zongwang Li. Espn: Memory-efficient multi-vector infor-
 727 mation retrieval. In *Proceedings of the 2024 ACM SIGPLAN International Symposium on Memory*
 728 *Management*, pp. 95–107, 2024.

729

730 Jiamin Su, Yibo Yan, Zhuoran Gao, Han Zhang, Xiang Liu, and Xuming Hu. Cafes: A col-
 731 laborative multi-agent framework for multi-granular multimodal essay scoring. *arXiv preprint*
 732 *arXiv:2505.13965*, 2025a.

733

734 Jianlin Su, Jiarun Cao, Weijie Liu, and Yangyiwen Ou. Whitening sentence representations for
 735 better semantics and faster retrieval. *arXiv preprint arXiv:2103.15316*, 2021.

736

737 Zhaochen Su, Peng Xia, Hangyu Guo, Zhenhua Liu, Yan Ma, Xiaoye Qu, Jiaqi Liu, Yanshu Li,
 738 Kaide Zeng, Zhengyuan Yang, et al. Thinking with images for multimodal reasoning: Founda-
 739 tions, methods, and future frontiers. *arXiv preprint arXiv:2506.23918*, 2025b.

740

741 Ryota Tanaka, Taichi Iki, Taku Hasegawa, Kyosuke Nishida, Kuniko Saito, and Jun Suzuki.
 742 Vdocrag: Retrieval-augmented generation over visually-rich documents. In *Proceedings of the*
 743 *Computer Vision and Pattern Recognition Conference*, pp. 24827–24837, 2025.

744

745 Naftali Tishby and Noga Zaslavsky. Deep learning and the information bottleneck principle. In
 746 *2015 ieee information theory workshop (itw)*, pp. 1–5. Ieee, 2015.

747

748 Naftali Tishby, Fernando C Pereira, and William Bialek. The information bottleneck method. *arXiv*
 749 *preprint physics/0004057*, 2000.

750

751 Jihene Tmamna, Emna Ben Ayed, Rahma Fourati, Mandar Gogate, Tughrul Arslan, Amir Hussain,
 752 and Mounir Ben Ayed. Pruning deep neural networks for green energy-efficient models: A survey.
 753 *Cognitive Computation*, 16(6):2931–2952, 2024.

754

755 Liang Wang, Nan Yang, Xiaolong Huang, Linjun Yang, Rangan Majumder, and Furu Wei. Improv-
 756 ing text embeddings with large language models. *arXiv preprint arXiv:2401.00368*, 2023.

757

758 Shuai Wang, Shengyao Zhuang, Bevan Koopman, and Guido Zuccon. 2d matryoshka training for in-
 759 formation retrieval. In *Proceedings of the 48th International ACM SIGIR Conference on Research*
 760 *and Development in Information Retrieval*, pp. 3125–3134, 2025a.

761

762 Tianshi Wang, Fengling Li, Lei Zhu, Jingjing Li, Zheng Zhang, and Heng Tao Shen. Cross-modal
 763 retrieval: a systematic review of methods and future directions. *Proceedings of the IEEE*, 2025b.

756 Yiqi Wang, Wentao Chen, Xiaotian Han, Xudong Lin, Haiteng Zhao, Yongfei Liu, Bohan Zhai,
 757 Jianbo Yuan, Quanzeng You, and Hongxia Yang. Exploring the reasoning abilities of multimodal
 758 large language models (mllms): A comprehensive survey on emerging trends in multimodal rea-
 759 soning. *arXiv preprint arXiv:2401.06805*, 2024.

760 Zichen Wen, Yifeng Gao, Weijia Li, Conghui He, and Linfeng Zhang. Token pruning in multimodal
 761 large language models: Are we solving the right problem? In *Findings of the Association for*
 762 *Computational Linguistics: ACL 2025*, pp. 15537–15549, Vienna, Austria, July 2025. Association
 763 for Computational Linguistics. ISBN 979-8-89176-256-5. doi: 10.18653/v1/2025.findings-acl.
 764 802. URL <https://aclanthology.org/2025.findings-acl.802/>.

765 Shiguang Wu, Wenda Wei, Mengqi Zhang, Zhumin Chen, Jun Ma, Zhaochun Ren, Maarten de Rijke,
 766 and Pengjie Ren. Generative retrieval as multi-vector dense retrieval. In *Proceedings of the 47th*
 767 *International ACM SIGIR Conference on Research and Development in Information Retrieval*,
 768 pp. 1828–1838, 2024.

769 Shitao Xiao, Zheng Liu, Peitian Zhang, Niklas Muennighoff, Defu Lian, and Jian-Yun Nie. C-pack:
 770 Packed resources for general chinese embeddings. In *Proceedings of the 47th international ACM*
 771 *SIGIR conference on research and development in information retrieval*, pp. 641–649, 2024.

772 Junlin Xie, Zhihong Chen, Ruifei Zhang, Xiang Wan, and Guanbin Li. Large multimodal agents: A
 773 survey. *arXiv preprint arXiv:2402.15116*, 2024.

774 Mengyao Xu, Gabriel Moreira, Ronay Ak, Radek Osmulski, Yauhen Babakhin, Zhiding Yu,
 775 Benedikt Schifferer, and Even Oldridge. Llama nemoretriever colembed: Top-performing text-
 776 image retrieval model. *arXiv preprint arXiv:2507.05513*, 2025a.

777 Mingjun Xu, Zehui Wang, Hengxing Cai, and Renxin Zhong. A multi-granularity retrieval frame-
 778 work for visually-rich documents. *arXiv preprint arXiv:2505.01457*, 2025b.

779 Yibo Yan and Joey Lee. Georeasoner: Reasoning on geospatially grounded context for natural
 780 language understanding. In *Proceedings of the 33rd ACM international conference on information*
 781 *and knowledge management*, pp. 4163–4167, 2024.

782 Yibo Yan, Jiamin Su, Jianxiang He, Fangteng Fu, Xu Zheng, Yuanhuiyi Lyu, Kun Wang, Shen Wang,
 783 Qingsong Wen, and Xuming Hu. A survey of mathematical reasoning in the era of multimodal
 784 large language model: Benchmark, method & challenges. *arXiv preprint arXiv:2412.11936*,
 785 2024a.

786 Yibo Yan, Shen Wang, Jiahao Huo, Hang Li, Boyan Li, Jiamin Su, Xiong Gao, Yi-Fan Zhang, Tian-
 787 long Xu, Zhendong Chu, et al. Errorradar: Benchmarking complex mathematical reasoning of
 788 multimodal large language models via error detection. *arXiv preprint arXiv:2410.04509*, 2024b.

789 Yibo Yan, Haomin Wen, Siru Zhong, Wei Chen, Haodong Chen, Qingsong Wen, Roger Zimmer-
 790 mann, and Yuxuan Liang. Urbanclip: Learning text-enhanced urban region profiling with con-
 791 trastive language-image pretraining from the web. In *Proceedings of the ACM Web Conference*
 792 2024, pp. 4006–4017, 2024c.

793 Yibo Yan, Shen Wang, Jiahao Huo, Jingheng Ye, Zhendong Chu, Xuming Hu, Philip S Yu, Carla
 794 Gomes, Bart Selman, and Qingsong Wen. Position: Multimodal large language models can sig-
 795 nificantly advance scientific reasoning. *arXiv preprint arXiv:2502.02871*, 2025a.

796 Yibo Yan, Shen Wang, Jiahao Huo, Philip S Yu, Xuming Hu, and Qingsong Wen. Mathagent:
 797 Leveraging a mixture-of-math-agent framework for real-world multimodal mathematical error
 798 detection. *arXiv preprint arXiv:2503.18132*, 2025b.

799 Weihao Ye, Qiong Wu, Wenhao Lin, and Yiyi Zhou. Fit and prune: Fast and training-free visual
 800 token pruning for multi-modal large language models. In *Proceedings of the AAAI Conference on*
 801 *Artificial Intelligence*, volume 39, pp. 22128–22136, 2025a.

802 Xubing Ye, Yukang Gan, Yixiao Ge, Xiao-Ping Zhang, and Yansong Tang. Atp-llava: Adaptive
 803 token pruning for large vision language models. In *Proceedings of the Computer Vision and*
 804 *Pattern Recognition Conference*, pp. 24972–24982, 2025b.

810 Jinsung Yoon, Raj Sinha, Sercan O Arik, and Tomas Pfister. Matryoshka-adaptor: Unsupervised and
 811 supervised tuning for smaller embedding dimensions. *arXiv preprint arXiv:2407.20243*, 2024.
 812

813 Rufai Yusuf Zakari, Jim Wilson Owusu, Hailin Wang, Ke Qin, Zaharaddeen Karami Lawal, and
 814 Yuezhou Dong. Vqa and visual reasoning: An overview of recent datasets, methods and chal-
 815 lenges. *arXiv preprint arXiv:2212.13296*, 2022.

816 Jiaxin Zhang, Wentao Yang, Songxuan Lai, Zecheng Xie, and Lianwen Jin. Dockylin: A large mul-
 817 timodal model for visual document understanding with efficient visual slimming. In *Proceedings*
 818 *of the AAAI Conference on Artificial Intelligence*, volume 39, pp. 9923–9932, 2025a.
 819

820 Junyuan Zhang, Qintong Zhang, Bin Wang, Linke Ouyang, Zichen Wen, Ying Li, Ka-Ho Chow,
 821 Conghui He, and Wentao Zhang. Ocr hinders rag: Evaluating the cascading impact of ocr on
 822 retrieval-augmented generation. *arXiv preprint arXiv:2412.02592*, 2024a.

823 Kun Zhang, Jingyu Li, Zhe Li, and Jingjing Zhang. Composed multi-modal retrieval: A survey of
 824 approaches and applications. *arXiv preprint arXiv:2503.01334*, 2025b.
 825

826 Qizhe Zhang, Aosong Cheng, Ming Lu, Zhiyong Zhuo, Minqi Wang, Jiajun Cao, Shaobo Guo,
 827 Qi She, and Shanghang Zhang. [cls] attention is all you need for training-free visual token prun-
 828 ing: Make vlm inference faster. *arXiv e-prints*, pp. arXiv–2412, 2024b.

829 Qizhe Zhang, Aosong Cheng, Ming Lu, Renrui Zhang, Zhiyong Zhuo, Jiajun Cao, Shaobo Guo,
 830 Qi She, and Shanghang Zhang. Beyond text-visual attention: Exploiting visual cues for effective
 831 token pruning in vlms. *arXiv preprint arXiv:2412.01818*, 2025c.

832 Xin Zhang, Yanzhao Zhang, Wen Xie, Mingxin Li, Ziqi Dai, Dingkun Long, Pengjun Xie, Meishan
 833 Zhang, Wenjie Li, and Min Zhang. Gme: Improving universal multimodal retrieval by multimodal
 834 llms. *arXiv preprint arXiv:2412.16855*, 2024c.
 835

836 Yuan Zhang, Chun-Kai Fan, Junpeng Ma, Wenzhao Zheng, Tao Huang, Kuan Cheng, Denis Gu-
 837 dovskiy, Tomoyuki Okuno, Yohei Nakata, Kurt Keutzer, et al. Sparsevlm: Visual token sparsifi-
 838 cation for efficient vision-language model inference. *arXiv preprint arXiv:2410.04417*, 2024d.

839 Kening Zheng, Junkai Chen, Yibo Yan, Xin Zou, and Xuming Hu. Reefknot: A comprehensive
 840 benchmark for relation hallucination evaluation, analysis and mitigation in multimodal large lan-
 841 guage models. *arXiv preprint arXiv:2408.09429*, 2024.
 842

843 Xu Zheng, Ziqiao Weng, Yuanhuiyi Lyu, Lutao Jiang, Haiwei Xue, Bin Ren, Danda Paudel, Nicu
 844 Sebe, Luc Van Gool, and Xuming Hu. Retrieval augmented generation and understanding in
 845 vision: A survey and new outlook. *arXiv preprint arXiv:2503.18016*, 2025.

846 Siru Zhong, Xixuan Hao, Yibo Yan, Ying Zhang, Yangqiu Song, and Yuxuan Liang. Urbancross:
 847 Enhancing satellite image-text retrieval with cross-domain adaptation. In *Proceedings of the 32nd*
 848 *ACM International Conference on Multimedia*, pp. 6307–6315, 2024.

849 Guanyu Zhou, Yibo Yan, Xin Zou, Kun Wang, Aiwei Liu, and Xuming Hu. Mitigating modal-
 850 ity prior-induced hallucinations in multimodal large language models via deciphering attention
 851 causality. *arXiv preprint arXiv:2410.04780*, 2024.
 852

853 Junyi Zhu, Shuochen Liu, Yu Yu, Bo Tang, Yibo Yan, Zhiyu Li, Feiyu Xiong, Tong Xu, and
 854 Matthew B Blaschko. Fastmem: fast memorization of prompt improves context awareness of
 855 large language models. *arXiv preprint arXiv:2406.16069*, 2024.

856 Xingchen Zou, Yibo Yan, Xixuan Hao, Yuehong Hu, Haomin Wen, Erdong Liu, Junbo Zhang, Yong
 857 Li, Tianrui Li, Yu Zheng, et al. Deep learning for cross-domain data fusion in urban computing:
 858 Taxonomy, advances, and outlook. *Information Fusion*, 113:102606, 2025.
 859

860

861

862

863

Technical Appendices and Supplements

A MORE RELATED WORK

A.1 LARGE VISION-LANGUAGE MODELS

Large Vision-Language Models (LVLMs) have recently revolutionized a multitude of fields, including visual question answering (Borisova et al., 2025; Zakari et al., 2022; Jang et al., 2025), urban sensing (Zou et al., 2025; Yan et al., 2024c; Yan & Lee, 2024; Hou et al., 2025b), multimodal reasoning (Wang et al., 2024; Yan et al., 2025a; 2024a; Su et al., 2025b; Yan et al., 2024b), multimodal retrieval (Lin et al., 2024; Lu & Tang, 2025; Kagaya et al., 2024; Zhong et al., 2024), and visual document understanding (Li et al., 2024c; Zhang et al., 2025a; Ding et al., 2024; Hu et al., 2024a;b). The architecture of these models generally follows several key paradigms. The first involves connecting a pre-trained vision encoder (e.g., ViT) and a LLM via a lightweight projection module, as seen in models like BLIP-2 (Li et al., 2023). A second paradigm consists of end-to-end trained models that process visual and textual inputs within a unified architecture, such as PaliGemma (Beyer et al., 2024). A third, highly effective approach involves freezing the core vision and language backbones and fine-tuning lightweight adapters (e.g., LoRA) to bridge the modalities, a strategy popularized by LLaVA (Li et al., 2024b;a). Furthermore, recent research is actively optimizing these models for critical real-world requirements, such as minimizing hallucination (Bai et al., 2024; Zhou et al., 2024; Zheng et al., 2024; Zhu et al., 2024), enabling agent-based interaction (Xie et al., 2024; Yan et al., 2025b; Su et al., 2025a; Durante et al., 2024), and enhancing interpretability (Lin et al., 2025; Huo et al., 2024; 2025; Huang et al., 2025) and safety (Fang et al., 2025; Chen et al., 2025; Liu et al., 2025a). The multi-vector models evaluated in our work are built upon such powerful LVLMs; for instance, ColQwen (Faysse et al., 2024) and ColNomic (NomicAI, 2025) are based on the Qwen2.5-VL series (Bai et al., 2025), one of the leading open-source LVLMs, while Jina Embeddings v4 (Günther et al., 2025) further leverages this foundation to implement a unified training paradigm for both single-vector and multi-vector outputs.

A.2 PRUNING IN LVLMs

The extensive length of visual token sequences in LVLMs poses significant computational challenges, motivating a surge of research in token compression (Cheng et al., 2024a; Tmamna et al., 2024; Ye et al., 2025a). These training-free methods primarily fall into two paradigms. The first is **instruction-centric pruning** (Hou et al., 2025a; Huang et al., 2024; Federici et al., 2024), which leverages query-document interaction. Methods like FastV (Chen et al., 2024b) and Sparse-VLM (Zhang et al., 2024d) identify redundant visual tokens by analyzing the cross-attention scores between textual instructions and visual patches. While effective for tasks like VQA, this paradigm is fundamentally *incompatible with the offline indexing phase of VDR*, as it requires a query to determine token importance. The second paradigm is **vision-centric compression** (Ye et al., 2025b; Jiang et al., 2024a), which is query-agnostic and thus more suitable for offline processing. This category includes token merging approaches like ToMe (Bolya et al., 2022), which progressively combines similar tokens, and token pruning methods like FasterVLM (Zhang et al., 2024b), which uses the attention scores of the [CLS] token within the vision encoder to rank and discard less salient patches. However, these vision-centric methods often suffer from their own limitations, such as information dilution from merging or retaining redundant tokens due to the concentrated nature of attention. Crucially, most pruning strategies are designed for and evaluated on generative tasks, and their direct application to the offline retrieval setting is underexplored (Lassance et al., 2023; Acquavia et al., 2023; Liu et al., 2024). They are *not tailored to preserve the fine-grained, discriminative features essential for the late-interaction mechanism in multi-vector retrieval*.

A.3 EFFICIENT DOCUMENT RETRIEVAL

The pursuit of efficiency in multi-vector retrieval (Wu et al., 2024; Park et al., 2025; Shrestha et al., 2024; Bian et al., 2025; Scheerer et al., 2025), a challenge amplified in the visual domain, has been addressed through two main orthogonal approaches: **Dimension Reduction** and **Token Reduction**. Dimension reduction aims to shrink the size of each embedding vector (Su et al., 2021; Yoon et al., 2024; Wang et al., 2025a). A prominent example is ColBERTv2 (Santhanam et al., 2021),

which employed product quantization to compress embeddings. This principle was later inherited by ColPali (Faysse et al., 2024), which uses a simpler projection layer for the same purpose. The second, more impactful approach is token reduction, which focuses on decreasing the number of vectors stored per document and can be divided into pruning and merging strategies (Liu et al., 2023; Mao et al., 2025; Cheng et al., 2024b). However, recent empirical studies (Ma et al., 2025) have highlighted that token merging strategies, which aggregate multiple embeddings into a smaller set of representative vectors (e.g., via spatial pooling or semantic clustering (Clavié et al., 2024)), are considered more appropriate for the offline VDR context as they retain information from all patches. Our work, **DocPruner**, revisits the pruning paradigm by introducing a novel *adaptive, query-agnostic mechanism that sidesteps the pitfalls of static pruning*, offering a storage-efficient alternative to merging-based approaches.

918
919
920
921
922
923
924
925
926
927
928
929
930
931
932
933
934
935
936
937
938
939
940
941
942
943
944
945
946
947
948
949
950
951
952
953
954
955
956
957
958
959
960
961
962
963
964
965
966
967
968
969
970
971

B ALGORITHM WORKFLOW

We formalize the complete workflow of our proposed framework in two distinct algorithms. **Algorithm 1** details the offline indexing phase, where **DocPruner** generates a compact set of document embeddings by adaptively pruning patches based on their attention-derived importance scores. Subsequently, **Algorithm 2** illustrates the online retrieval phase, where the final relevance score is efficiently computed via a **MaxSim** operation using this pruned set of embeddings.

Algorithm 1: The DocPruner Adaptive Pruning (Offline Indexing Phase)

Input: A document page d ;
 A VLM encoder $\Phi(\cdot)$ that outputs patch embeddings and attention weights;
 A sensitivity controller hyperparameter k .
Output: A pruned set of patch embeddings \mathbf{D}'

Output: A pruned set of patch embeddings D_d .

```

/* Step 0: VLM Forward Pass
{D_d, A(L)} ← Φ(d) // Extract embeddings D_d = {dj}j=1L_d and final layer attention
A(L)

/* Step 1: Quantifying Patch Importance */
Let g be the index of the global token (e.g., [EOS])
Initialize an empty list of importance scores I_d
for j ← 1 to L_d do
  | Āg,j(L) ← 1/H ∑h=1H Ah,g,j(L)
  | I(dj) ← Āg,j(L) // Importance is attention to patch j (Eq. 2)
  | Append I(dj) to I_d
end

/* Step 2: Adaptive Thresholding */
μ_d ← 1/L_d ∑j=1L_d I(dj) // Calculate mean importance (Eq. 3)
σ_d ← √(1/L_d ∑j=1L_d (I(dj) - μ_d)2) // Calculate std dev of importance (Eq. 4)
τ_d ← μ_d + k · σ_d // Define the document-specific threshold

D'_d ← {}
for j ← 1 to L_d do
  | if I(dj) > τ_d then
  |   | D'_d ← D'_d ∪ {dj} // Keep patch if importance > threshold (Eq. 5)
  | end
end

/* Step 3: Finalizing with Robustness Guarantee */
if D'_d = ∅ then
  | j* ← arg maxj ∈ {1, ..., L_d} I(dj)
  | D'_d ← {dj*} // Keep the single most important patch (Eq. 6)
else
  | D'_d ← D'_d
end

return D'_d

```

1026
 1027
 1028
 1029
 1030
 1031
 1032
 1033
 1034
 1035
 1036
 1037
 1038
 1039
 1040
 1041
 1042

Algorithm 2: Scoring with Pruned Embeddings (Online Retrieval Phase)

1043 **Input:** A textual query q ;
 1044 The pruned document embedding set \mathbf{D}'_d (from Algorithm 1);
 1045 A VLM encoder $\Phi(\cdot)$ for query encoding.
 1046 **Output:** The relevance score $s'(q, d)$.

1047

```

1048 /* Step 1: Encode Query                                     */
1049 Q  $\leftarrow \Phi(q)$                                      // Encode  $q$  into token embeddings  $\mathbf{Q} = \{\mathbf{q}_i\}_{i=1}^{L_q}$ 
1050 /* Step 2: Compute Score with Pruned Embeddings           */
1051  $s'(q, d) \leftarrow 0$ 
1052 for  $\mathbf{q}_i \in \mathbf{Q}$  do
1053    $\text{max\_sim} \leftarrow -\infty$ 
1054   for  $\mathbf{d}_j \in \mathbf{D}'_d$  do
1055      $\text{sim} \leftarrow \mathbf{q}_i^\top \mathbf{d}_j$ 
1056     if  $\text{sim} > \text{max\_sim}$  then
1057        $\text{max\_sim} \leftarrow \text{sim}$ 
1058     end
1059   end
1060    $s'(q, d) \leftarrow s'(q, d) + \text{max\_sim}$     // Aggregate max similarity per query token (Sec
1061     3.2.3)
1062 end
1063 return  $s'(q, d)$ 
1064
1065
1066
1067
1068
1069
1070
1071
1072
1073
1074
1075
1076
1077
1078
1079
```

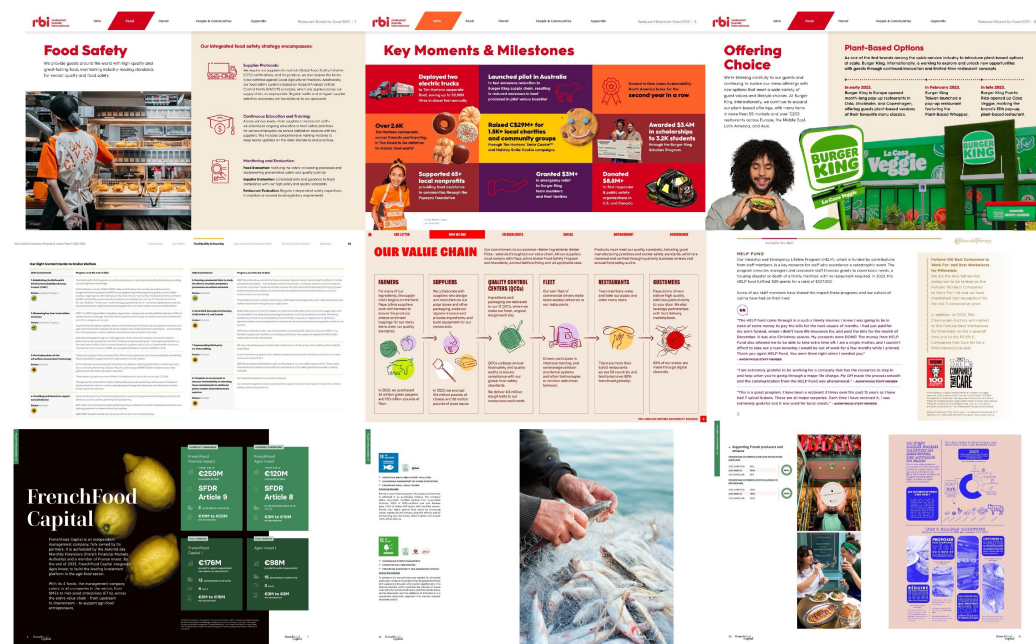
1080 C DETAILS OF BENCHMARKS

1081
 1082 This section provides detailed descriptions of the benchmarks used in our evaluation to validate the
 1083 performance of DocPruner.

1084 C.1 ViDOR-EV2 BENCHMARK

1085 The ViDOR-EV2 benchmark (Macé et al., 2025) was designed to address the saturation of its pre-
 1086 predecessor, ViDOR-EV1 (Fayolle et al., 2024), where top models were achieving near-perfect scores. It in-
 1087 troduces more realistic and challenging retrieval scenarios by incorporating several key features: (1) **1088 Blind Contextual Querying**, where query generation models have limited context, forcing them to
 1089 create non-extractive questions that better mimic real user behavior; (2) **1090 Long and Cross-Document**
 1091 **1092 Queries**, which require models to retrieve information from multiple pages or across different docu-
 1093 ments; and (3) a **1094 Hybrid Generation Process**, combining synthetic query generation with extensive
 1095 human-in-the-loop filtering to ensure high query quality. The benchmark comprises four diverse
 1096 datasets: `esg-reports-v2`², `biomedical-lectures-v2`³, `economics-reports-v2`⁴, and `esg-reports-human-
 1097 labeled-v2`⁵, making it a robust testbed for model generalization.

1098 Illustration of visual document examples from ViDOR-EV2 benchmark (Macé et al., 2025) can be
 1099 seen in Figures 6, 7, and 8.



1100
 1101 **1102 Figure 6:** Illustration of visual document examples from *ESG* and *ESG-human* datasets (The latter is fully
 1103 labelled by hand, and has no overlap of queries with its synthetic counterpart). They focus on the theme of
 1104 **1105 ESG reports from the fast food industry.**

1106
 1107 ²https://huggingface.co/datasets/vidore/esg_reports_v2

1108 ³https://huggingface.co/datasets/vidore/biomedical_lectures_v2

1109 ⁴https://huggingface.co/datasets/vidore/economics_reports_v2

1110 ⁵https://huggingface.co/datasets/vidore/esg_reports_human_labeled_v2

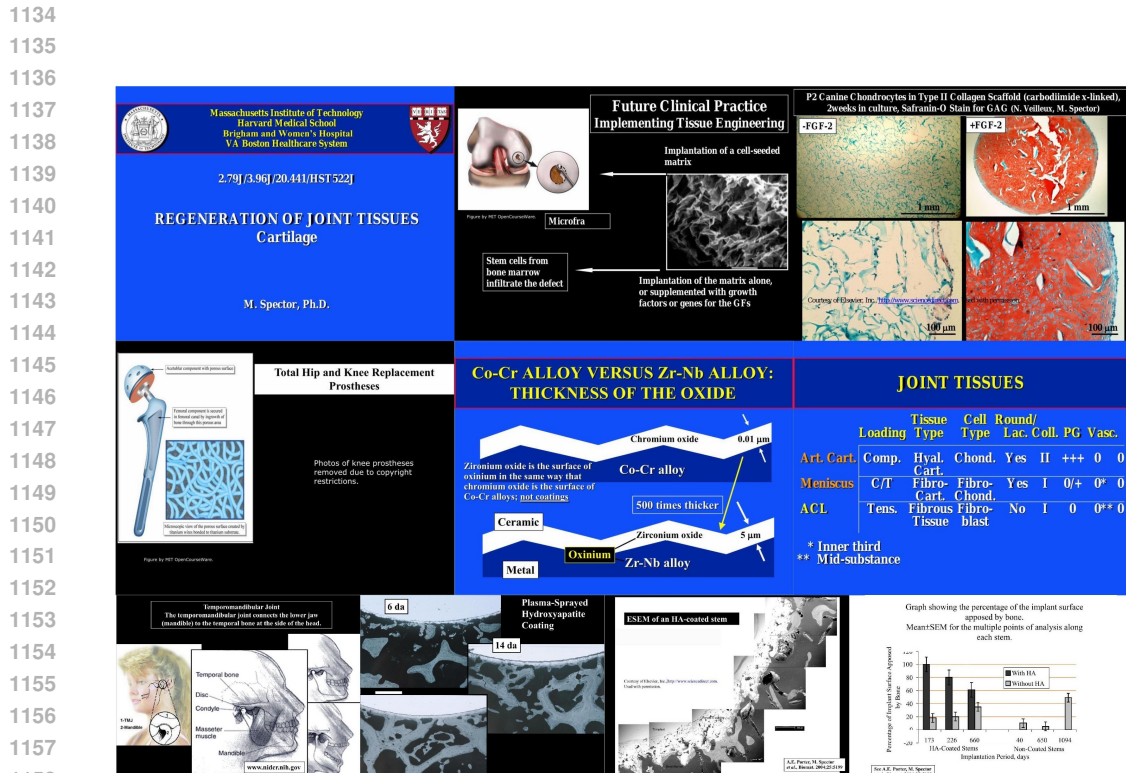


Figure 7: Illustration of visual document examples from *Biomedical Lectures* datasets. It focuses on the theme of **MIT courses in anatomy** (precisely tissue interactions).

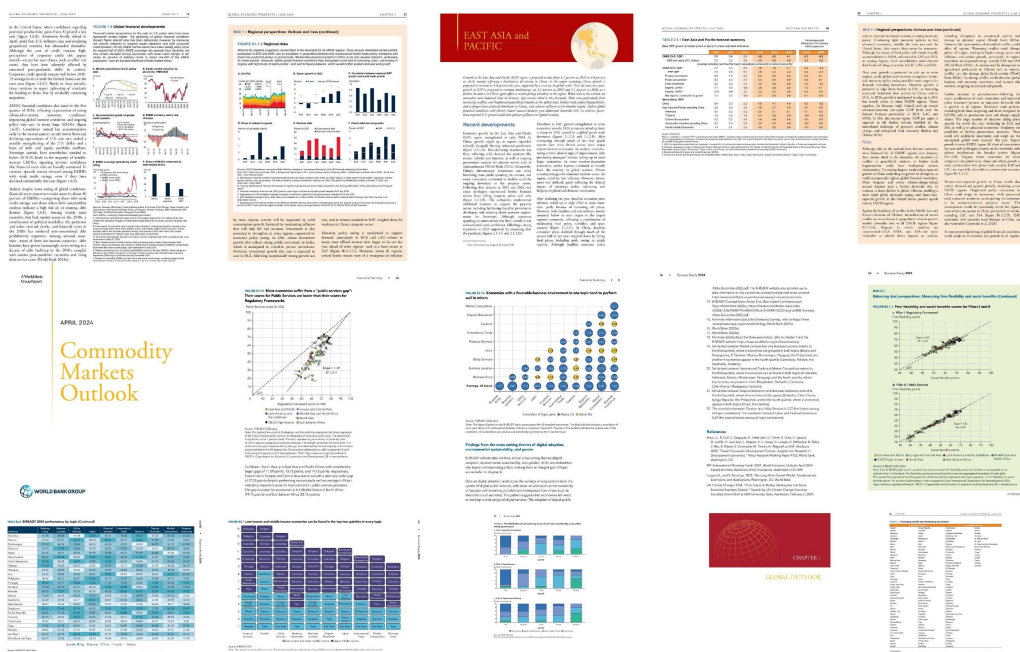


Figure 8: Illustration of visual document examples from *Economics Reports* datasets. It focuses on the theme of **World economic reports from 2024**.

1188
1189

C.2 JINAVDR-BENCH

1190 JinaVDR-Bench was introduced alongside Jina Embeddings v4 (Günther et al., 2025) to evaluate a
 1191 new generation of unified embedding models capable of producing both single-vector (dense) and
 1192 multi-vector representations from a single architecture. The benchmark is notable for its breadth,
 1193 covering a wide array of document types and retrieval tasks. Its datasets include academic
 1194 papers (Astro-ph), financial reports (DocILE, DeepForm), presentation slides (SlideVQA), technical
 1195 manuals, and infographics (InfographicsVQA), among others. This diversity tests a model’s ability
 1196 to handle documents with varying layouts, languages (it includes multilingual splits), and content
 1197 (e.g., text-heavy, table-rich, or figure-dominant). By providing a standardized evaluation across
 1198 these heterogeneous sources, JinaVDR-Bench serves as a comprehensive tool for assessing the
 1199 versatility and robustness of VDR models. To evaluate the multilingual generalization of DocPruner,
 1200 we choose europeana-de-news⁶, beverages-catalogue-ru⁷, shanghai-master-plan⁸, and automobile-
 1201 catalogue-jp⁹ for German, Russian, Chinese, and Japanese visual documents, respectively.

1202 Illustration of visual document examples from JinaVDR-Bench (Günther et al., 2025) can be seen
 1203 in Figures 9, 10, 11, and 12.



1224 **Figure 9:** Illustration of visual document examples from *German* datasets. It focuses on the records of the
 1225 European online collection by selecting scans of **German news articles**.

1226

C.3 VISUALIZATION OF PRUNED DOCUMENT CASES

1227

1228 This section illustrate the visual examples of pruned documents, as depicted by Figures 13 and 14.

1229

1230

1231

1232

1233

1234

1235

1236

1237

1238

⁶<https://huggingface.co/datasets/jinaai/europeana-de-news>

⁷https://huggingface.co/datasets/jinaai/beverages_catalogue_ru

⁸https://huggingface.co/datasets/jinaai/shanghai_master_plan

⁹https://huggingface.co/datasets/jinaai/automobile_catalogue_jp

1242

1243

1244

1245

1246

1247

1248

1249

1250

1251

1252

1253

1254

1255

1256

1257

1258

1259

1260

1261

1262



Figure 10: Illustration of visual document examples from *Russian* datasets. It focuses on the **beverage catalogs** on Google search and downloading PDFs.

1263

1264

1265

1266

1267

1268

1269

1270

1271

1272

1273

1274

1275

1276

1277

1278

1279

1280

1281

1282

1283

1284

1285

1286

1287

1288

1289

1290

1291



Figure 11: Illustration of visual document examples from *Chinese* datasets. It focuses on the theme of **Shanghai master plan document** taken from ([Shanghai Municipal People's Government Urban Planning and Land Resource Administration Bureau, 2018](http://www.shapl.gov.cn)).

1292

1293

1294

1295

1296

1297

1298

1299

1300

1301

1302

1303

1304

1305

1306

1307

1308

1309

1310

1311

1312

1313

1314

1315

1316

1317

1318

1319

1320

1321

1322

1323

1324

1325

1326

1327

1328

1329

1330

1331

1332

1333

1334

1335

1336

1337

1338

1339

1340

1341

1342

1343

1344

1345

1346

1347

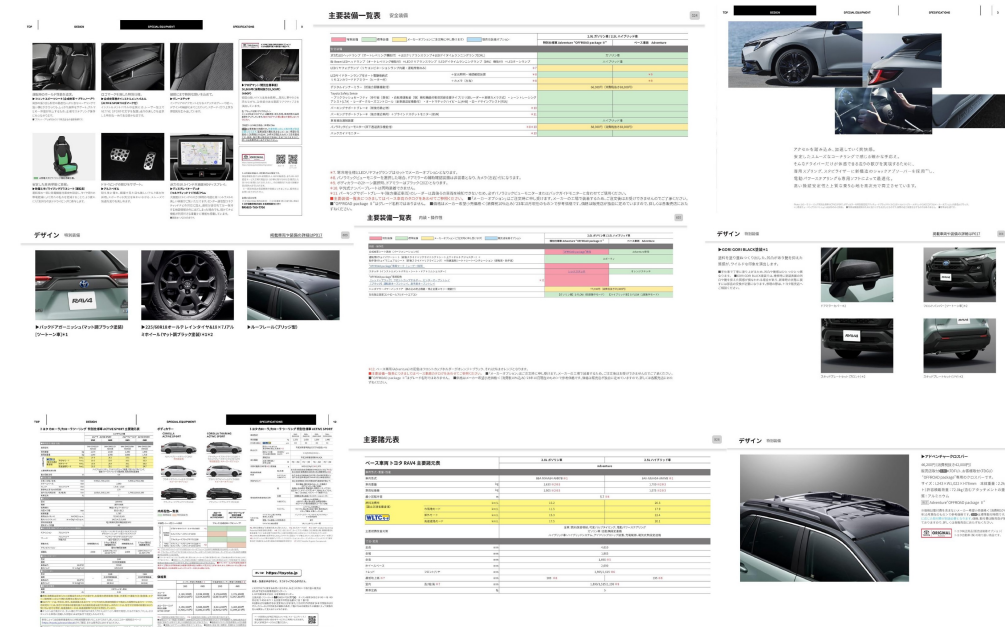


Figure 12: Illustration of visual document examples from *Japanese* datasets. It focuses on the theme of **marketing document** from Toyota Japanese website.

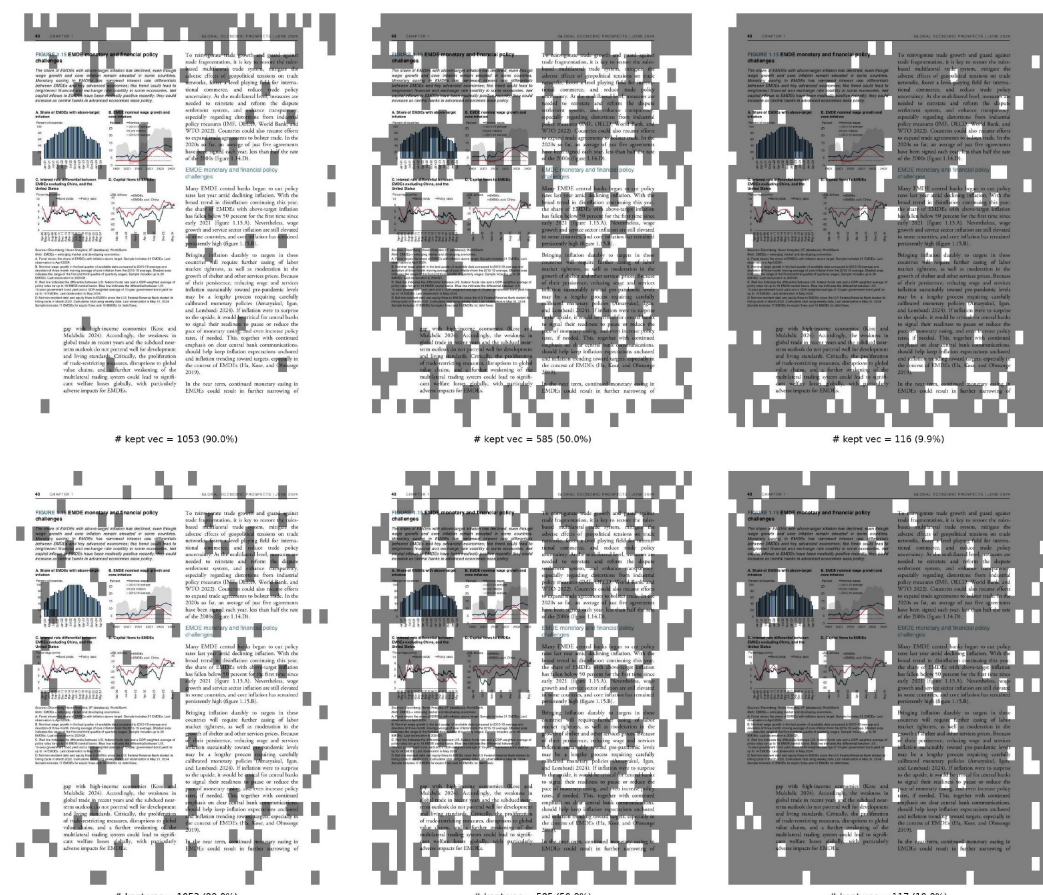


Figure 13: Illustration of visual document example one. Comparison of fixed-ratio pruning (*top row*) and random pruning (*bottom row*) at ratios of 10%, 50%, and 90% (*from left to right*). Gray patches are pruned and excluded from the multi-vector computation.



Figure 14: Illustration of visual document example two. Comparison of fixed-ratio pruning (top row) and random pruning (bottom row) at ratios of 10%, 50%, and 90% (from left to right). Gray patches are pruned and excluded from the multi-vector computation.

1387
1388
1389
1390
1391
1392
1393
1394
1395
1396
1397
1398
1399
1400
1401
1402
1403

1404 D DETAILS OF BASELINES

1405
 1406 This section provides a detailed description of the implementation logic and hyperparameter settings
 1407 for the baseline methods evaluated in Section 4.1. For each baseline, we empirically explored the
 1408 specified hyperparameter space and selected the configurations that yielded the most representative
 1409 performance trade-offs for presentation in our main results.
 1410

1411 D.1 MERGING-BASED METHODS

1412 D.1.1 SEM-CLUSTER

1413
 1414 **Implementation Logic.** This method performs semantic merging of patch embeddings. For each
 1415 document, it first normalizes all patch embeddings. Then, it computes a pairwise distance matrix
 1416 based on cosine similarity ($\text{distance} = 1 - \text{cosine_similarity}$). Using this matrix, it
 1417 applies hierarchical agglomerative clustering with the 'ward' linkage method. The total number
 1418 of patch embeddings is reduced by a *merging factor*, which determines the target number of clus-
 1419 ters (*i.e.*, $\text{num_clusters} = \text{num_patches} / \text{merging_factor}$). Finally, the embeddings
 1420 within each resulting cluster are averaged to produce a single centroid embedding, forming the new,
 1421 smaller set of representations for the document.
 1422

1423 Hyperparameters.

1424
 1425 • **Merging Factor:** Defines the ratio by which the number of patch embeddings is reduced.
 1426 A higher factor results in fewer clusters and thus more aggressive merging.
 1427
 1428 – *Selection Range:* {2, 4, 9, 16, 25}.

1429 D.1.2 1D-POOLING

1430
 1431 **Implementation Logic.** This strategy treats the patch embeddings as a 1D sequence. It groups
 1432 consecutive embeddings into non-overlapping windows of size equal to the *merging factor*. If the
 1433 total number of patches is not divisible by the factor, the sequence is padded with zero vectors to
 1434 ensure complete windows. The embeddings within each window are then averaged to create a single
 1435 merged embedding. This effectively downsamples the sequence of patch embeddings.
 1436

1437 Hyperparameters.

1438
 1439 • **Merging Factor:** Specifies the size of the pooling window, *i.e.*, the number of sequential
 1440 patch embeddings to be averaged into one.
 1441
 1442 – *Selection Range:* {2, 4, 9, 16, 25}.

1443 D.1.3 2D-POOLING

1444
 1445 **Implementation Logic.** This method assumes a spatial arrangement of patches. The patch em-
 1446 beddings are first organized into a 2D grid that approximates their original spatial layout in the
 1447 document image. This grid is padded with zero vectors to ensure its dimensions are divisible by the
 1448 pooling kernel size. A 2D average pooling operation is then applied. The *merging factor*, which
 1449 must be a perfect square, defines the area of the pooling window (*e.g.*, a factor of 4 corresponds
 1450 to a 2x2 kernel). A mask is used during pooling to correctly normalize the averages, ensuring that
 1451 padded areas do not contribute to the final merged embeddings.
 1452

1453 Hyperparameters.

1454
 1455 • **Merging Factor:** Defines the area of the 2D pooling window.
 1456
 1457 – *Selection Range:* {4, 9, 16, 25}.

1458 D.2 PRUNING-BASED METHODS

1459

1460 D.2.1 RANDOM

1461

Implementation Logic. This naive baseline discards patch embeddings without considering their content. For each document, a specified *pruning ratio* of the total patch embeddings are selected uniformly at random and removed from the set. To ensure at least one patch remains, the implementation prevents pruning all patches even if the ratio is 1.0. This serves as a fundamental benchmark to gauge the performance loss from non-informed pruning.

1466

1467 **Hyperparameters.**

1468

- **Pruning Ratio:** A float between 0.0 and 1.0 that specifies the fraction of patch embeddings to be randomly discarded.
 - *Selection Range:* $\{0.1, 0.3, 0.5, 0.7, 0.9\}$.

1471

1473 D.2.2 ATTENTION-PLUS-SIMILARITY

1474

Implementation Logic. This adaptive method computes a composite score for each patch to decide whether to prune it. The score is a weighted sum of two components: (1) an **importance score**, derived from the attention weight the global [EOS] token pays to the patch, and (2) a **representativeness score**, calculated as the cosine similarity between the patch embedding and the [EOS] embedding. The final score is pruned using an adaptive threshold calculated as $\mu + k \cdot \sigma$, where μ and σ are the statistics of the composite scores for that document. The results presented in the paper were based on an empirical grid search over all hyperparameter combinations, selecting the optimal α for $k = 0$ and $k = 1$ respectively to show representative results.

1482

1483 **Hyperparameters.**

1484

- **Adaptation Factor (k):** A coefficient that controls the strictness of the dynamic pruning threshold. A higher value leads to a more aggressive pruning.
 - *Selection Range:* $\{-0.5, -0.25, 0, 0.25, 0.5, 1\}$.
- **Weighting Factor (α):** A float between 0.0 and 1.0 that balances the contribution of the importance score (attention) and the representativeness score (similarity).
 - *Selection Range:* $\{0.1, 0.3, 0.5, 0.7, 0.9\}$.

1491

1492 D.2.3 PIVOT-THRESHOLD

1493

Implementation Logic. This advanced adaptive baseline employs a two-stage pruning process. It first identifies an “important set” of patches by applying an adaptive attention-based threshold ($\mu + k \cdot \sigma$ of [EOS]-to-patch attention scores), similar to the core mechanism of **DocPruner**. Within this important set, it selects a fixed *pivot num* of patches as “pivots”. For the remaining non-pivot patches in the important set, it calculates a duplication score, defined as the maximum cosine similarity to any of the pivots. A second adaptive threshold ($\mu_{\text{dup}} + k_{\text{dup}} \cdot \sigma_{\text{dup}}$ of these duplication scores) is then used to prune non-pivot patches that are deemed too similar to the pivots. We found $k_{\text{dup}} = 1$ and *pivot_num* = 10 were consistently optimal via empirical search. Therefore, the results presented fix these two hyperparameters and show the performance trade-off by varying the adaptation factor k .

1503

1504 **Hyperparameters.**

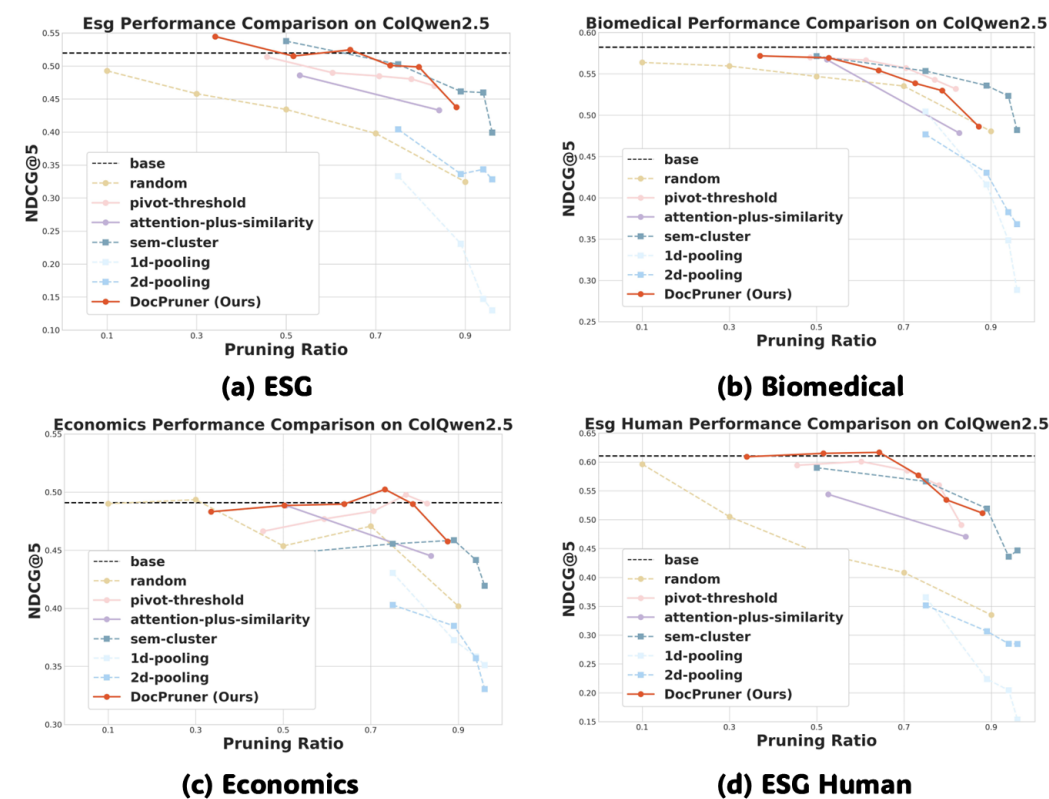
1505

- **Adaptation Factor (k):** Controls the threshold for initial importance-based filtering stage.
 - *Selection Range:* $\{-0.5, -0.25, 0, 0.25, 0.5, 1\}$.
- **De-duplication Factor (k_{dup}):** Controls the similarity threshold for the second stage.
 - *Selection Range:* $\{-0.5, -0.25, 0, 0.25, 0.5, 1\}$.
- **Pivot Num:** The number of pivot tokens to select from the important set for the de-duplication stage.

1512 – *Selection Range*: $\{5, 10, 15, 20\}$.
1513
1514
1515
1516
1517
1518
1519
1520
1521
1522
1523
1524
1525
1526
1527
1528
1529
1530
1531
1532
1533
1534
1535
1536
1537
1538
1539
1540
1541
1542
1543
1544
1545
1546
1547
1548
1549
1550
1551
1552
1553
1554
1555
1556
1557
1558
1559
1560
1561
1562
1563
1564
1565

1566 E MORE EXPERIMENTAL ANALYSIS
15671568 E.1 MORE EXPERIMENT ON ViDOR-E-V2
1569

1570 Performance comparison (nDCG@5) between DocPruner and baselines on ViDOR-E-V2 benchmark
1571 across four datasets on **ColQwen2.5**, **ColNomic**, and **Jina Embedding V4** can be seen in Figures
1572 **15**, **16**, and **17**, respectively. Pruning ratio distribution of DocPruner on **ColQwen2.5**, **ColNomic**,
1573 and **Jina Embedding V4** can be seen in Figures **18**, **19**, and **20**, respectively.



1600 **Figure 15:** Performance comparison (nDCG@5) of **ColQwen2.5** between DocPruner and baselines on
1601 ViDOR-E-V2 benchmark across four datasets.

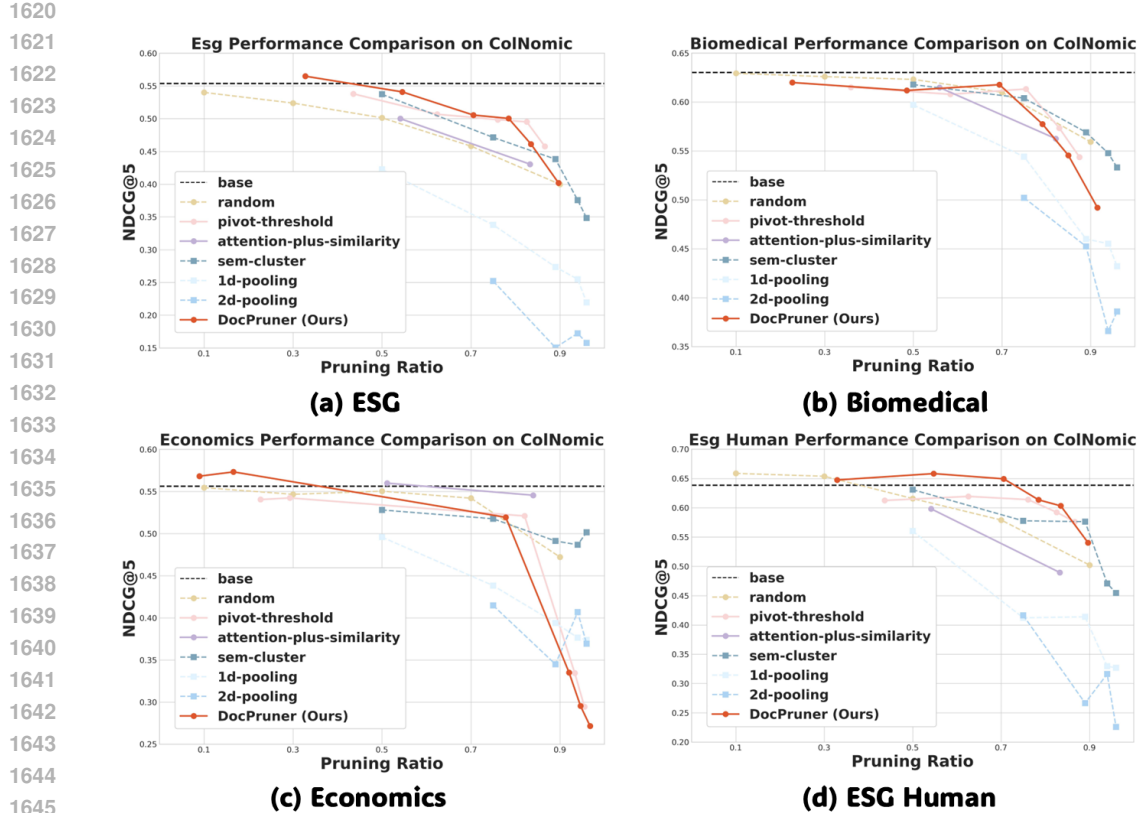


Figure 16: Performance comparison (nDCG@5) of ColNomic between DocPruner and baselines on ViDoRe-V2 benchmark across four datasets.

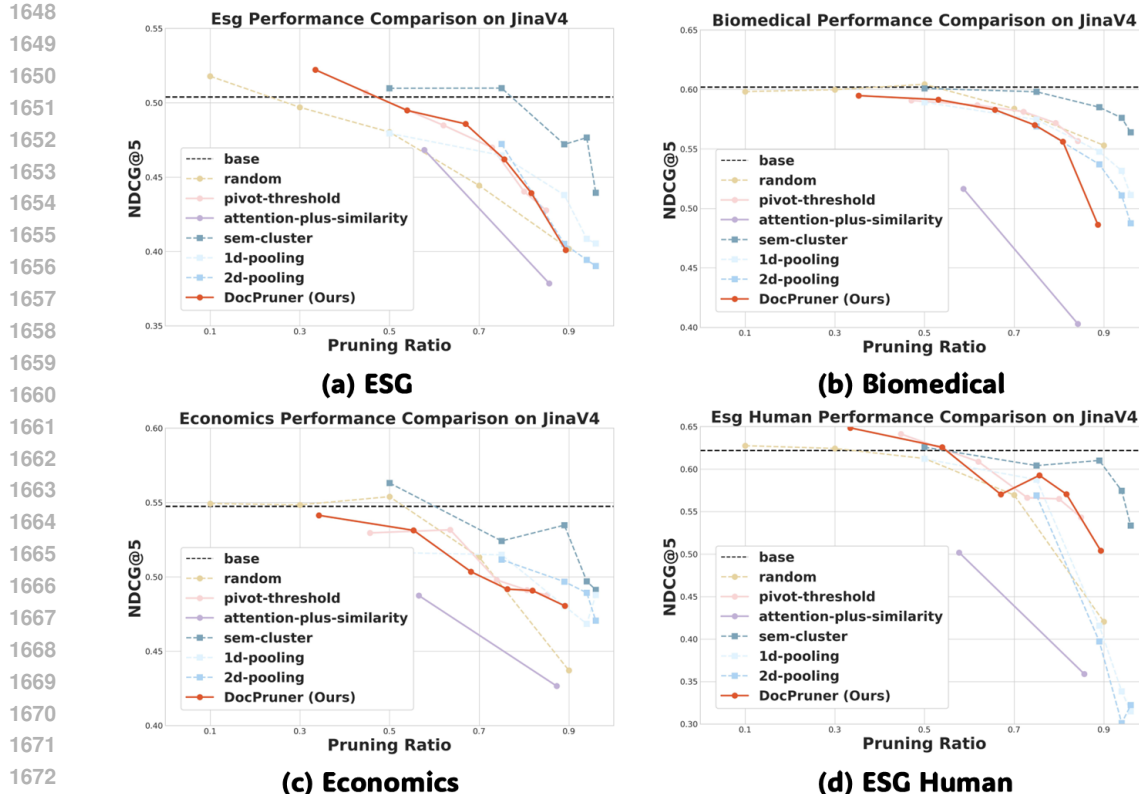


Figure 17: Performance comparison (nDCG@5) of Jina Embedding V4 between DocPruner and baselines on ViDoRe-V2 benchmark across four datasets.

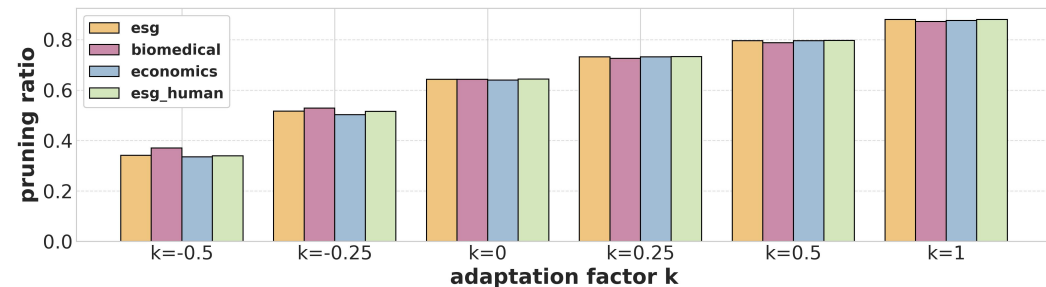


Figure 18: Pruning ratio distribution of ColQwen2.5 using DocPruner across four datasets of ViDiRe-V2 over a *adaptation factor k* range of {-0.5, -0.25, 0, 0.25, 0.5, 1}.

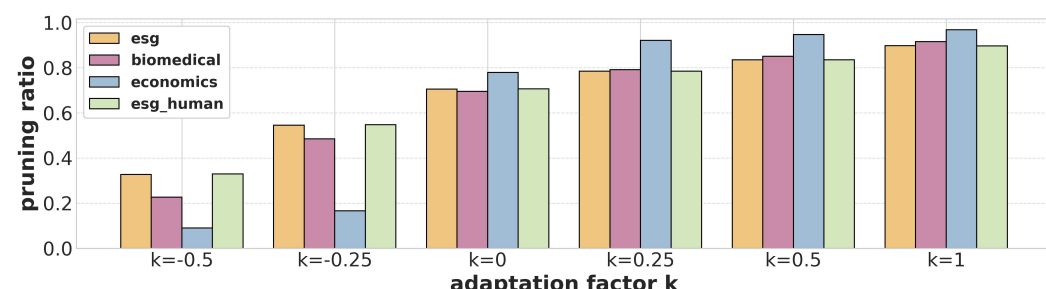


Figure 19: Pruning ratio distribution of ColNomic using DocPruner across four datasets of ViDiRe-V2 over a *adaptation factor k* range of {-0.5, -0.25, 0, 0.25, 0.5, 1}.

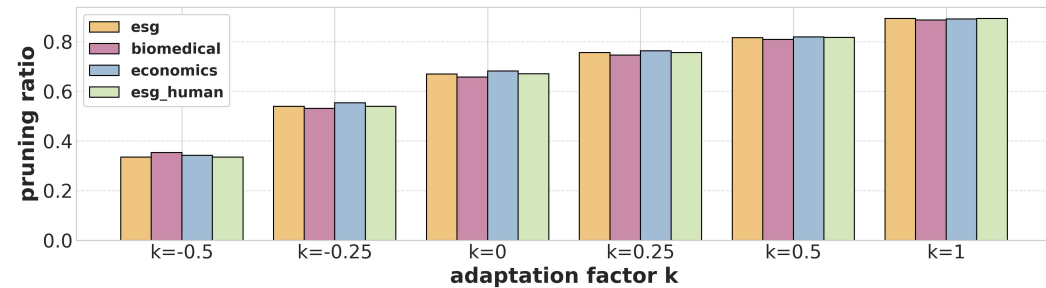


Figure 20: Pruning ratio distribution of Jina Embedding V4 using DocPruner across four datasets of ViDiRe-V2 over a *adaptation factor k* range of {-0.5, -0.25, 0, 0.25, 0.5, 1}.

E.2 MORE EXPERIMENT ON JINAVDR

Performance comparison (nDCG@5) between DocPruner and baselines on JinaVDR benchmark across four multilingual datasets on **ColQwen2.5**, **ColNomic**, and **Jina Embedding V4** can be seen in Figures 21, 22, and 23, respectively.

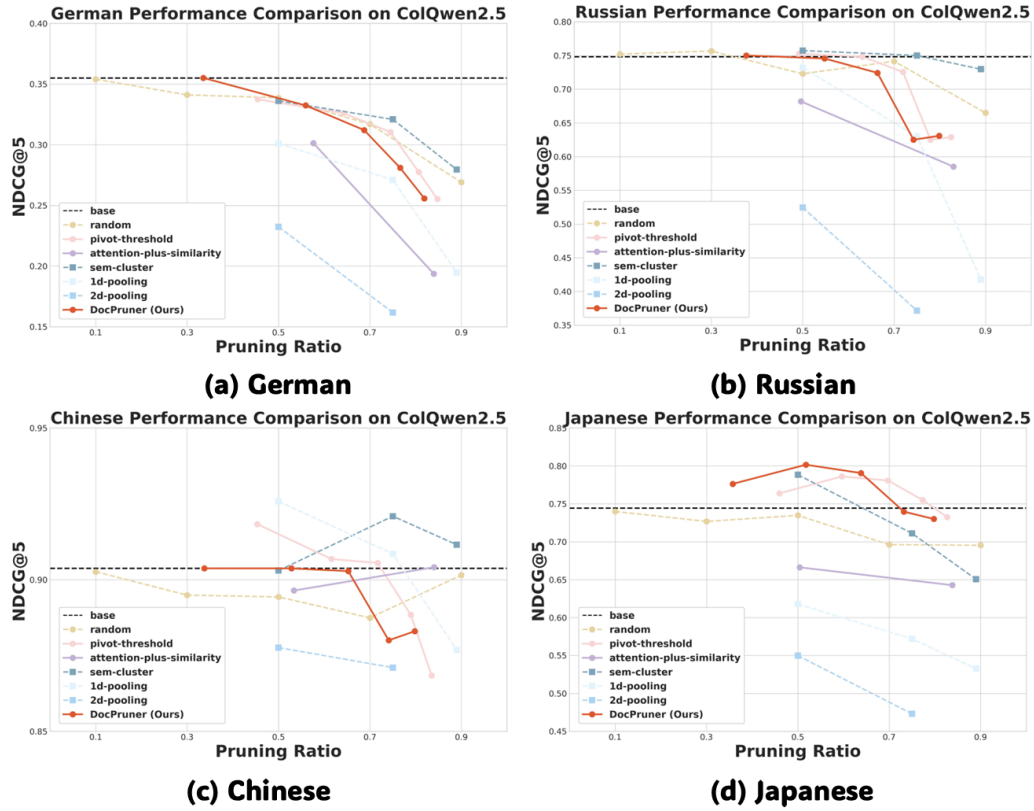


Figure 21: Performance comparison (nDCG@5) of **ColQwen2.5** between DocPruner and baselines on JinaVDR benchmark across four datasets.

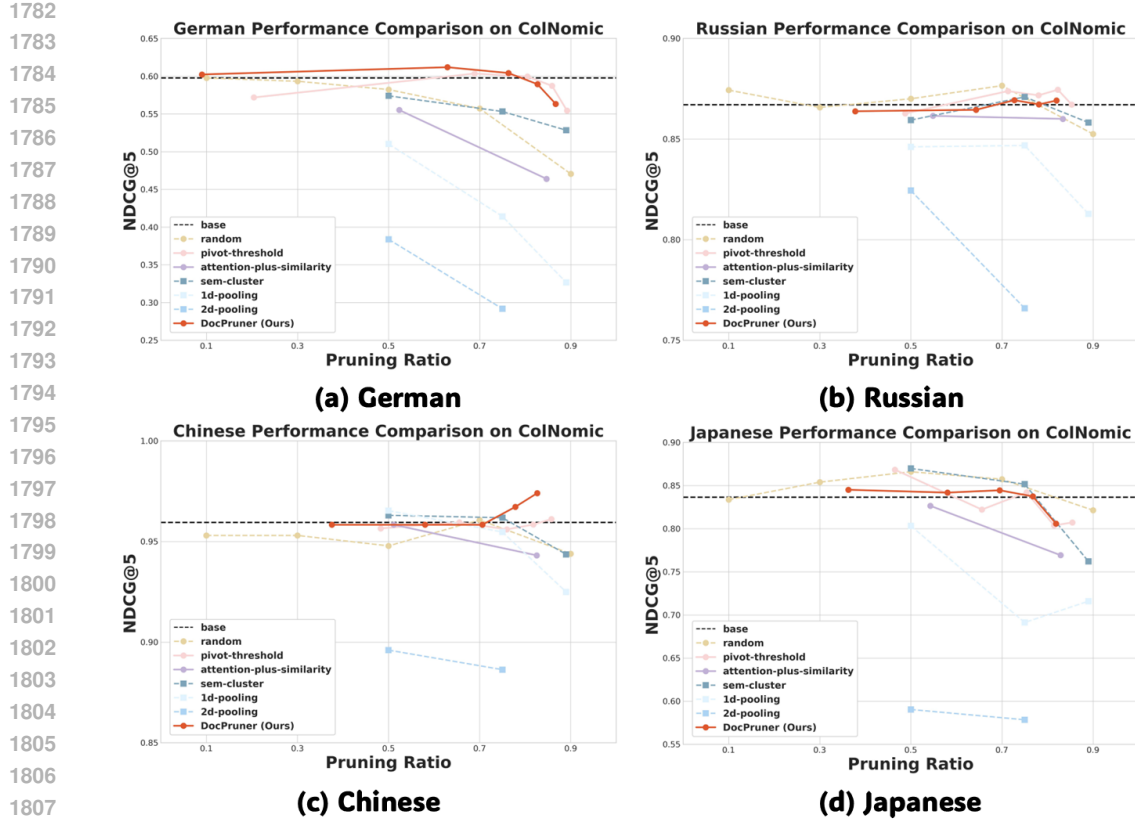


Figure 22: Performance comparison (nDCG@5) of ColNomic between DocPruner and baselines on JinaVDR benchmark across four datasets.

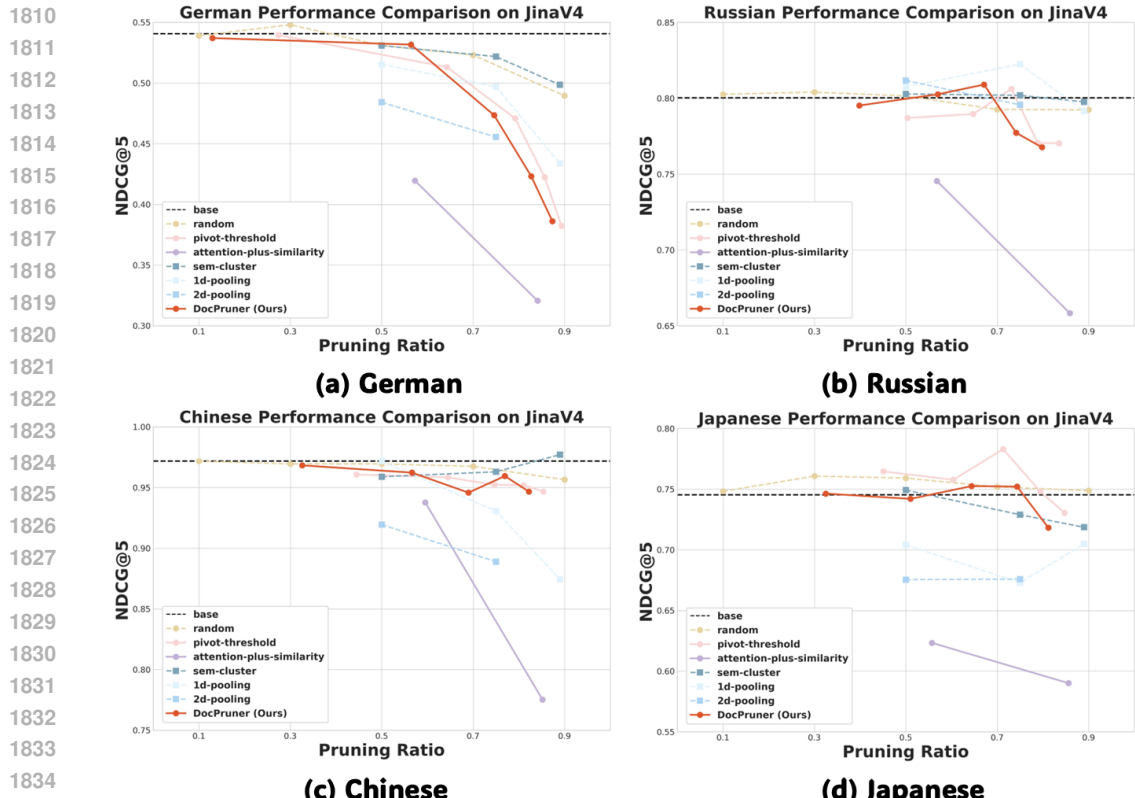


Figure 23: Performance comparison (nDCG@5) of Jina Embedding V4 between DocPruner and baselines on JinaVDR benchmark across four datasets.

1836

E.3 MORE VARIANT STUDY

1837

1838 Performance comparison (nDCG@5) between **DocPruner** and other variants on ViDoRe-V2 bench-
 1839 mark across four datasets on **ColQwen2.5**, **ColNomic**, and **Jina Embedding V4** can be seen in
 1840 Figure 24. The prompt used for evaluating attention-threshold-nfp is shown below.

1841

Prompt Template for attention-threshold-nfp

1842

1843

1844

1845

1846

1847

1848

1849

1850

1851

1852

1853

1854

1855

1856

1857

1858

1859

1860

1861

1862

1863

1864

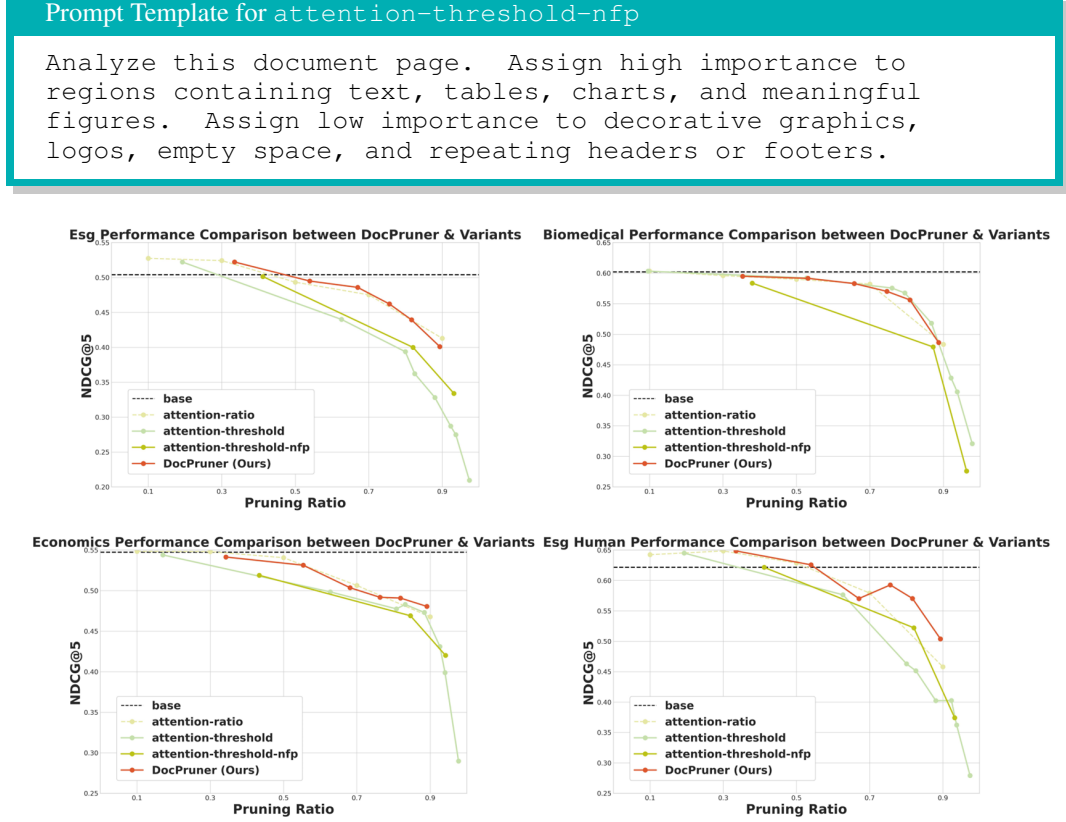
1865

1866

1867

1868

1869



1870
 1871
 1872
 1873
 1874
 1875
 1876
 1877
 1878
 1879
 1880
 1881
 1882
 1883
 1884
 1885
 1886
 1887
 1888
 1889

Figure 24: Performance comparison between **DocPruner** and other variants on ViDoRe-V2 benchmark across four datasets.

1890
1891

E.4 MORE ANALYSIS OF ADAPTATION FACTOR

1892
1893
1894
1895
1896
1897

The adaptation factor, k , is the central hyperparameter in the **DocPruner** framework, governing the delicate trade-off between storage compression and retrieval performance. Its significance lies not in setting a fixed threshold, but in modulating a dynamic one, $\tau_d = \mu_d + k \cdot \sigma_d$, which is tailored to the unique statistical properties of each document's attention score distribution. As illustrated in Figures 25-28, the interaction between k and the distribution's shape (characterized by its mean μ_d and standard deviation σ_d) is the key to **DocPruner**'s adaptive behavior.

1898
1899
1900
1901
1902
1903
1904

Furthermore, we observe a consistent principle across different VDR models (ColQwen2.5, Jina Embedding V4, and ColNomic). While the absolute attention scores and the specific shapes of the distributions may differ, each model fundamentally learns to assign higher attention to semantically meaningful regions. **DocPruner**'s statistical approach is robust to these model-specific variations, as it operates on the relative distribution of scores within each document. This intrinsic, document-relative nature is why a single k value (e.g., $k=-0.25$) can yield a desirable balance of $\sim 50\%$ compression and near-lossless performance across diverse models and datasets.

1905
1906
1907
1908
1909

In summary, the adaptation factor k is not a simple cutoff value but a sensitivity parameter. It leverages the statistical fingerprint of each document's attention distribution to determine the appropriate pruning intensity. This enables **DocPruner** to automatically apply a “one-size-fits-one” strategy: conservative pruning for information-rich pages and aggressive pruning for sparse ones, achieving a robust and efficient compression solution for real-world visual document retrieval.

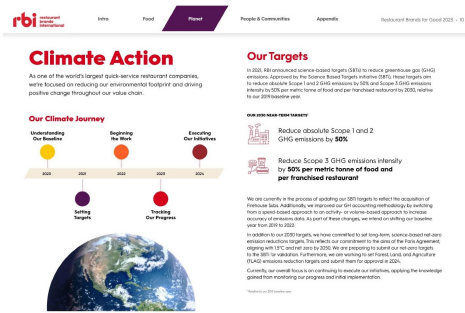
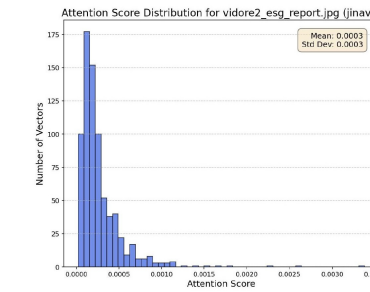
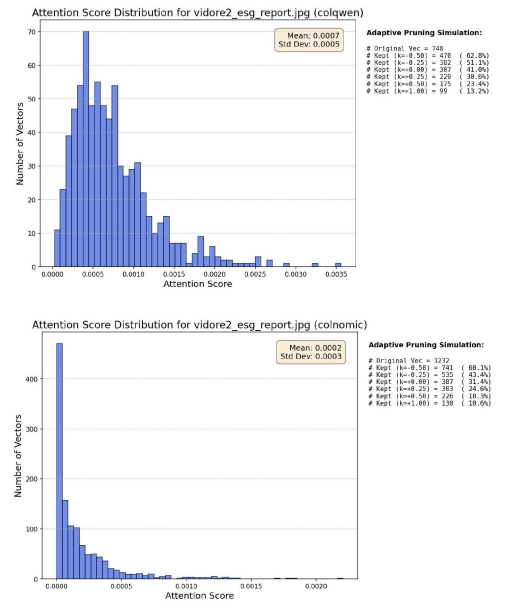
1910
1911
1912
1913
1914
1915
1916
1917
1918
1919
19201921
1922
1923
1924
1925
1926
1927
1928
19291930
1931
1932
1933
1934
1935
1936
1937
1938
1939
1940
1941
1942
1943

Figure 25: The attention score distribution and number of kept vectors (w.r.t. different adaption factor setting) of the representative document from *ESG* subset of *ViDoRe-V2*. The **raw document** is shown in top-left corner, and the rest represent histograms corresponding to **ColQwen2.5**, **Jina Embedding V4**, and **ColNomic**.



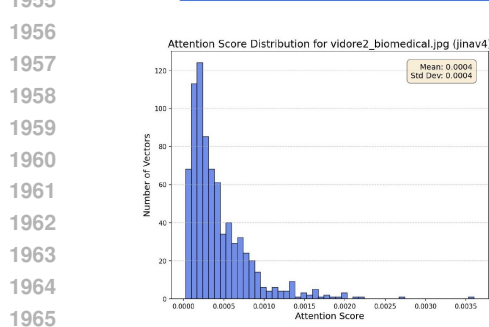


Figure 26: The attention score distribution and number of kept vectors (wrt. different adaption factor setting) of the representative document from *Biomedical* subset of ViDoRe-V2. The **raw document** is shown in top-left corner, and the rest represent histograms corresponding to **ColQwen2.5**, **Jina Embedding V4**, and **ColNomic**.

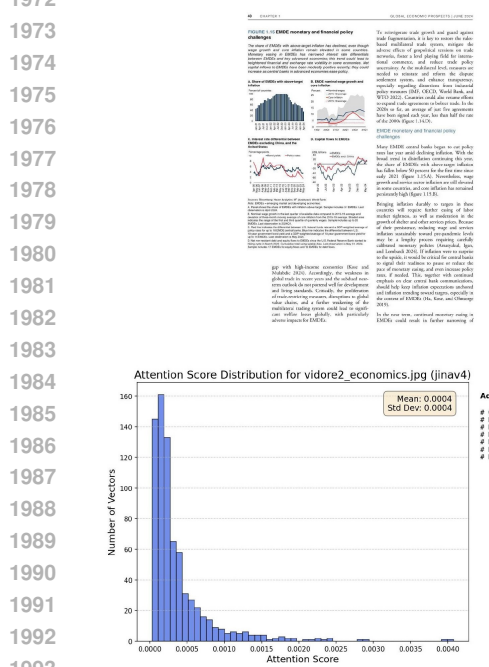
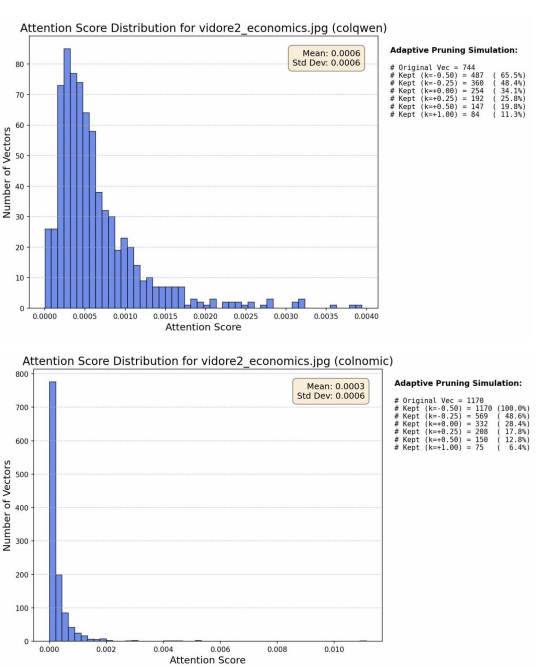
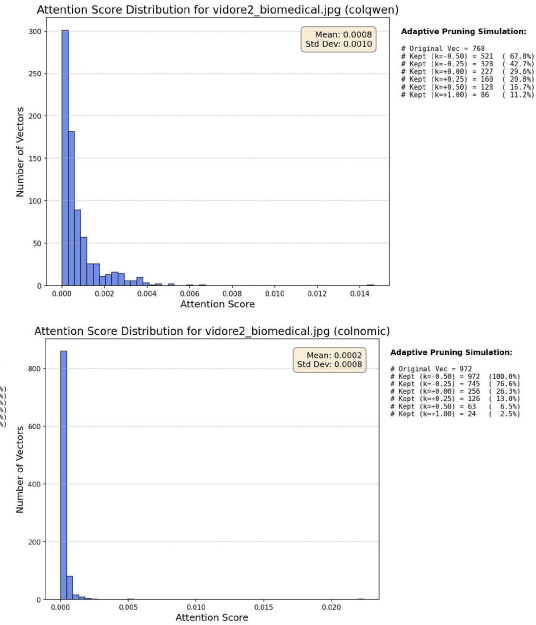


Figure 27: The attention score distribution and number of kept vectors (wrt. different adaption factor setting) of the representative document from *Economics* subset of ViDoRe-V2. The **raw document** is shown in top-left corner, and the rest represent histograms corresponding to **ColQwen2.5**, **Jina Embedding V4**, and **ColNomic**.



1998
1999
2000
2001
2002
2003
2004
2005
2006
2007
2008
2009
2010
2011
2012
2013
2014
2015
2016
2017
2018
2019
2020
2021
2022
2023
2024
2025
2026
2027
2028
2029
2030
2031
2032
2033
2034
2035
2036
2037
2038
2039
2040
2041
2042
2043
2044
2045
2046
2047
2048
2049
2050
2051

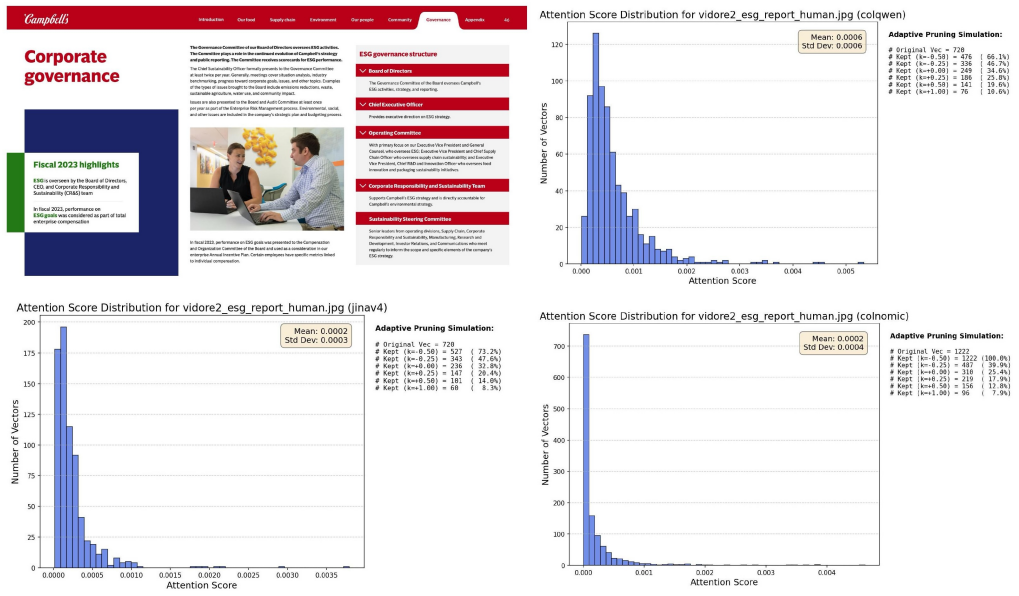


Figure 28: The attention score distribution and number of kept vectors (wrt. different adaption factor setting) of the representative document from *ESG Human* subset of ViDoRe-V2. The **raw document** is shown in top-left corner, and the rest represent histograms corresponding to **ColQwen2.5**, **Jina Embedding V4**, and **ColNomic**.

2052 **F BROADER IMPACT**
20532054 The development of **DocPruner** carries significant positive impacts that extend from the research
2055 community to industrial applications and ultimately to society at large. **DocPruner** addresses a
2056 critical, practical bottleneck in state-of-the-art VDR, and its implications can be understood on three
2057 distinct levels.2058 First, within the **academic and research community**, **DocPruner** encourages a paradigm shift.
2059 While much of the recent focus has been on scaling up models to achieve marginal gains in accuracy,
2060 our work highlights the paramount importance of computational and storage efficiency. By providing
2061 a simple yet effective framework for making powerful multi-vector models practical, we hope
2062 to inspire more research into resource-aware AI. This can enable researchers, particularly those in
2063 resource-constrained environments, to conduct larger-scale experiments and explore more complex
2064 VDR tasks that were previously computationally prohibitive. Our work serves as a proof-of-concept
2065 that “smarter” resource management can be as impactful as “bigger” models.2066 Second, for **industry and commercial applications**, **DocPruner** offers a direct and substantial eco-
2067 nomic benefit. The prohibitive storage costs associated with multi-vector embeddings are a major
2068 barrier to the widespread adoption of advanced VDR systems in enterprise settings. By reducing
2069 storage requirements by 50-60% with negligible performance loss, **DocPruner** makes it economi-
2070 cally feasible for businesses in sectors like legal, finance, healthcare, and e-commerce to deploy
2071 high-fidelity document search and analysis tools. This can unlock new efficiencies in knowledge
2072 management, accelerate workflows that rely on searching vast archives of visually-rich documents
2073 (e.g., contracts, financial reports, patent filings), and ultimately democratize access to state-of-the-art
2074 retrieval technology for a wider range of organizations.2075 Finally, on a broader **societal level**, the principles behind **DocPruner** contribute to making informa-
2076 tion more accessible and discoverable. Public institutions such as libraries, museums, and govern-
2077 ment archives are custodians of immense collections of digitized historical and cultural documents.
2078 The ability to affordably index and search these visual archives at a fine-grained level can empower
2079 educators, historians, and the general public, fostering new avenues for research and learning. By
2080 lowering the technological and financial barriers to building powerful search systems, our work
2081 can help preserve and unlock the value latent within our collective cultural and scientific heritage,
2082 contributing to a more informed and connected society.2083 **G THE USE OF LARGE LANGUAGE MODELS (LLMs)**
20842085 In the preparation of this manuscript, we utilized LLMs primarily for the purpose of language re-
2086 finement and improving the clarity and readability of our writing. The LLM was employed as an
2087 editing assistant to help polish sentence structures, correct grammatical errors, and ensure consis-
2088 tency in terminology. The core scientific ideas, the design and implementation of the **DocPruner**
2089 framework, the execution of experiments, and the analysis of the results were all conceived and
2090 conducted exclusively by the authors. The LLM’s role was strictly limited to enhancing the quality of
2091 the English prose and did not contribute to the intellectual content of the research.